2 Digital Image Fundamentals

Those who wish to succeed must ask the right preliminary questions.

Aristotle

Preview

The purpose of this chapter is to introduce several concepts related to digital images and some of the notation used throughout the book. Section 2.1 briefly summarizes the mechanics of the human visual system, including image formation in the eye and its capabilities for brightness adaptation and discrimination. Section 2.2 discusses light, other components of the electromagnetic spectrum, and their imaging characteristics. Section 2.3 discusses imaging sensors and how they are used to generate digital images. Section 2.4 introduces the concepts of uniform image sampling and gray-level quantization. Additional topics discussed in that section include digital image representation, the effects of varying the number of samples and gray levels in an image, some important phenomena associated with sampling, and techniques for image zooming and shrinking. Section 2.5 deals with some basic relationships between pixels that are used throughout the book. Finally, Section 2.6 defines the conditions for linear operations. As noted in that section, linear operators play a central role in the development of image processing techniques.

2.1 Elements of Visual Perception

Although the digital image processing field is built on a foundation of mathematical and probabilistic formulations, human intuition and analysis play a central role in the choice of one technique versus another, and this choice often is

made based on subjective, visual judgments. Hence, developing a basic understanding of human visual perception as a first step in our journey through this book is appropriate. Given the complexity and breadth of this topic, we can only aspire to cover the most rudimentary aspects of human vision. In particular, our interest lies in the mechanics and parameters related to how images are formed in the eye. We are interested in learning the physical limitations of human vision in terms of factors that also are used in our work with digital images. Thus, factors such as how human and electronic imaging compare in terms of resolution and ability to adapt to changes in illumination are not only interesting, they also are important from a practical point of view.

2.1.1 Structure of the Human Eye

Figure 2.1 shows a simplified horizontal cross section of the human eye. The eye is nearly a sphere, with an average diameter of approximately 20 mm. Three membranes enclose the eye: the *cornea* and *sclera* outer cover; the *choroid*; and the *retina*. The cornea is a tough, transparent tissue that covers the anterior

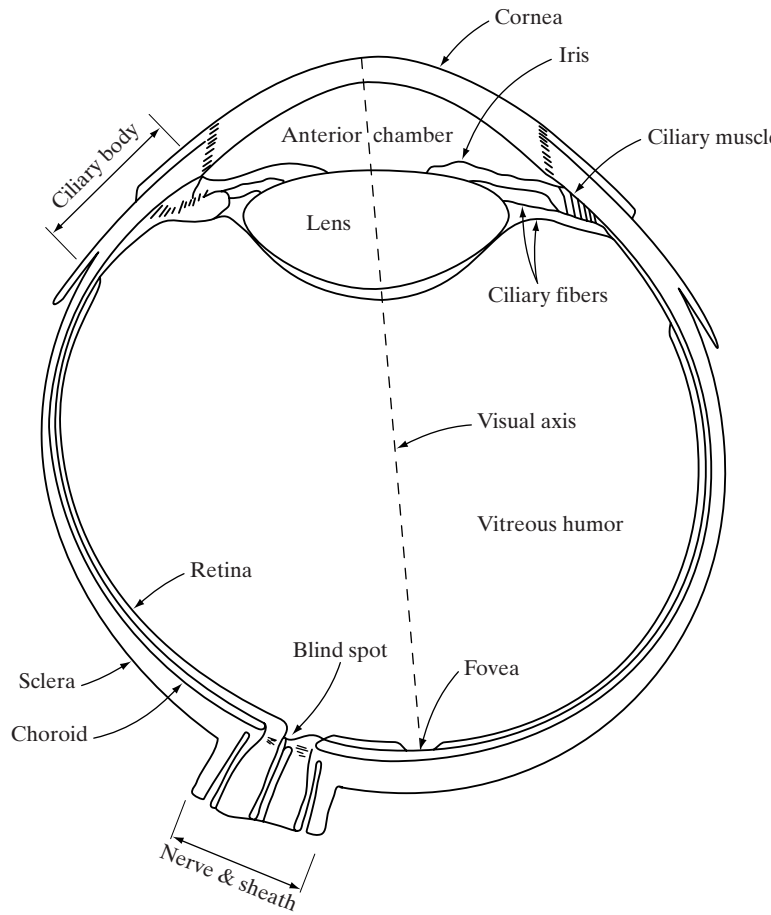

FIGURE 2.1 Simplified diagram of a cross section of the human eye.

surface of the eye. Continuous with the cornea, the sclera is an opaque membrane that encloses the remainder of the optic globe.

The choroid lies directly below the sclera. This membrane contains a network of blood vessels that serve as the major source of nutrition to the eye. Even superficial injury to the choroid, often not deemed serious, can lead to severe eye damage as a result of inflammation that restricts blood flow. The choroid coat is heavily pigmented and hence helps to reduce the amount of extraneous light entering the eye and the backscatter within the optical globe. At its anterior extreme, the choroid is divided into the *ciliary body* and the *iris diaphragm*. The latter contracts or expands to control the amount of light that enters the eye. The central opening of the iris (the *pupil*) varies in diameter from approximately 2 to 8 mm. The front of the iris contains the visible pigment of the eye, whereas the back contains a black pigment.

The *lens* is made up of concentric layers of fibrous cells and is suspended by fibers that attach to the ciliary body. It contains 60 to 70% water, about 6% fat, and more protein than any other tissue in the eye. The lens is colored by a slightly yellow pigmentation that increases with age. In extreme cases, excessive clouding of the lens, caused by the affliction commonly referred to as *cataracts*, can lead to poor color discrimination and loss of clear vision. The lens absorbs approximately 8% of the visible light spectrum, with relatively higher absorption at shorter wavelengths. Both infrared and ultraviolet light are absorbed appreciably by proteins within the lens structure and, in excessive amounts, can damage the eye.

The innermost membrane of the eye is the retina, which lines the inside of the wall's entire posterior portion. When the eye is properly focused, light from an object outside the eye is imaged on the retina. Pattern vision is afforded by the distribution of discrete light receptors over the surface of the retina. There are two classes of receptors: *cones* and *rods*. The cones in each eye number between 6 and 7 million. They are located primarily in the central portion of the retina, called the *fovea*, and are highly sensitive to color. Humans can resolve fine details with these cones largely because each one is connected to its own nerve end. Muscles controlling the eye rotate the eyeball until the image of an object of interest falls on the fovea. Cone vision is called *photopic* or bright-light vision.

The number of rods is much larger: Some 75 to 150 million are distributed over the retinal surface. The larger area of distribution and the fact that several rods are connected to a single nerve end reduce the amount of detail discernible by these receptors. Rods serve to give a general, overall picture of the field of view. They are not involved in color vision and are sensitive to low levels of illumination. For example, objects that appear brightly colored in daylight when seen by moonlight appear as colorless forms because only the rods are stimulated. This phenomenon is known as *scotopic* or dim-light vision.

Figure 2.2 shows the density of rods and cones for a cross section of the right eye passing through the region of emergence of the optic nerve from the eye. The absence of receptors in this area results in the so-called *blind spot* (see Fig. 2.1). Except for this region, the distribution of receptors is radially symmetric about the fovea. Receptor density is measured in degrees from the fovea (that is, in degrees off axis, as measured by the angle formed by the visual axis and a line passing through the center of the lens and intersecting the retina).

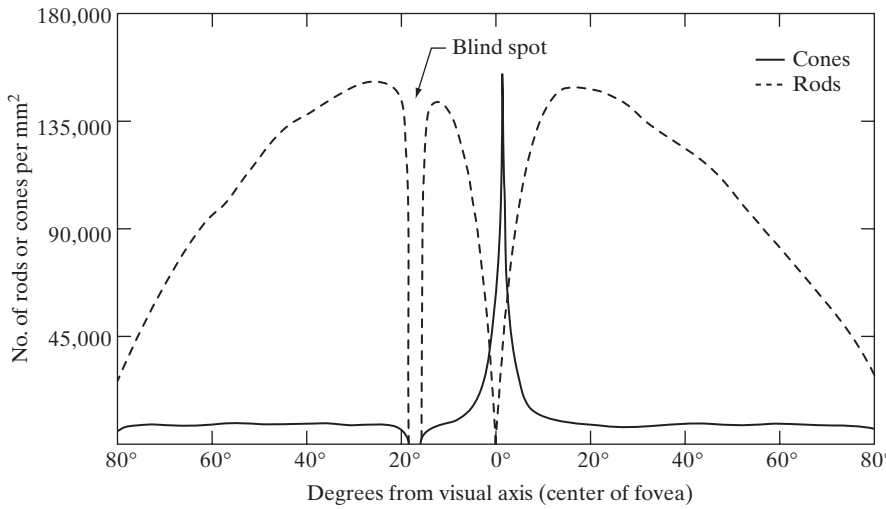

FIGURE 2.2 Distribution of rods and cones in the retina.

Note in Fig. 2.2 that cones are most dense in the center of the retina (in the center area of the fovea). Note also that rods increase in density from the center out to approximately 20° off axis and then decrease in density out to the extreme periphery of the retina.

The fovea itself is a circular indentation in the retina of about 1.5 mm in diameter. However, in terms of future discussions, talking about square or rectangular arrays of sensing elements is more useful. Thus, by taking some liberty in interpretation, we can view the fovea as a square sensor array of size 1.5 mm $\times$ 1.5 mm. The density of cones in that area of the retina is approximately 150,000 elements per mm^2. Based on these approximations, the number of cones in the region of highest acuity in the eye is about 337,000 elements. Just in terms of raw resolving power, a charge-coupled device (CCD) imaging chip of medium resolution can have this number of elements in a receptor array no larger than 5 mm $\times$ 5 mm. While the ability of humans to integrate intelligence and experience with vision makes this type of comparison dangerous. Keep in mind for future discussions that the basic ability of the eye to resolve detail is certainly within the realm of current electronic imaging sensors.

2.1.2 Image Formation in the Eye

The principal difference between the lens of the eye and an ordinary optical lens is that the former is flexible. As illustrated in Fig. 2.1, the radius of curvature of the anterior surface of the lens is greater than the radius of its posterior surface. The shape of the lens is controlled by tension in the fibers of the ciliary body. To focus on distant objects, the controlling muscles cause the lens to be relatively flattened. Similarly, these muscles allow the lens to become thicker in order to focus on objects near the eye.

The distance between the center of the lens and the retina (called the *focal length*) varies from approximately 17 mm to about 14 mm, as the refractive power of the lens increases from its minimum to its maximum. When the eye

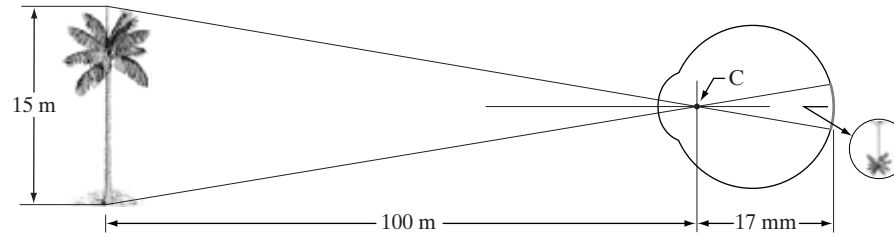

FIGURE 2.3 Graphical representation of the eye looking at a palm tree. Point *C* is the optical center of the lens.

focuses on an object farther away than about 3 m, the lens exhibits its lowest refractive power. When the eye focuses on a nearby object, the lens is most strongly refractive. This information makes it easy to calculate the size of the retinal image of any object. In Fig. 2.3, for example, the observer is looking at a tree 15 m high at a distance of 100 m. If h is the height in mm of that object in the retinal image, the geometry of Fig. 2.3 yields $15/100 = h/17$ or $h = 2.55$ mm. As indicated in Section 2.1.1, the retinal image is reflected primarily in the area of the fovea. Perception then takes place by the relative excitation of light receptors, which transform radiant energy into electrical impulses that are ultimately decoded by the brain.

2.1.3 Brightness Adaptation and Discrimination

Because digital images are displayed as a discrete set of intensities, the eye's ability to discriminate between different intensity levels is an important consideration in presenting image-processing results. The range of light intensity levels to which the human visual system can adapt is enormous—on the order of 10^{10}—from the scotopic threshold to the glare limit. Experimental evidence indicates that *subjective brightness* (intensity as *perceived* by the human visual system) is a logarithmic function of the light intensity incident on the eye. Figure 2.4, a plot of light intensity versus subjective brightness, illustrates this char-

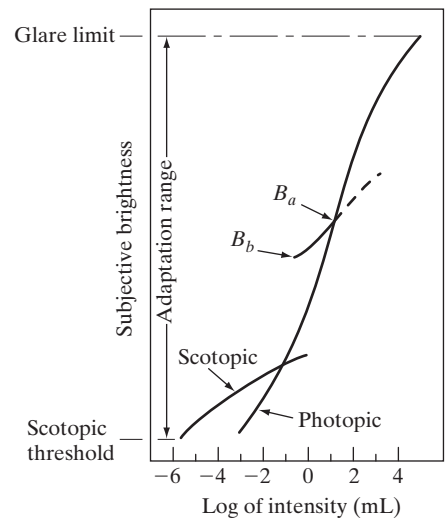

FIGURE 2.4 Range of subjective brightness sensations showing a particular adaptation level.

acteristic. The long solid curve represents the range of intensities to which the visual system can adapt. In photopic vision alone, the range is about 10^6. The transition from scotopic to photopic vision is gradual over the approximate range from 0.001 to 0.1 millilambert (−3 to −1 mL in the log scale), as the double branches of the adaptation curve in this range show.

The essential point in interpreting the impressive dynamic range depicted in Fig. 2.4 is that the visual system cannot operate over such a range *simultaneously.* Rather, it accomplishes this large variation by changes in its overall sensitivity, a phenomenon known as *brightness adaptation.* The total range of distinct intensity levels it can discriminate simultaneously is rather small when compared with the total adaptation range. For any given set of conditions, the current sensitivity level of the visual system is called the *brightness adaptation level,* which may correspond, for example, to brightness B_a in Fig. 2.4. The short intersecting curve represents the range of subjective brightness that the eye can perceive when adapted to this level. This range is rather restricted, having a level B_b at and below which all stimuli are perceived as indistinguishable blacks. The upper (dashed) portion of the curve is not actually restricted but, if extended too far, loses its meaning because much higher intensities would simply raise the adaptation level higher than B_a.

The ability of the eye to discriminate between *changes* in light intensity at any specific adaptation level is also of considerable interest. A classic experiment used to determine the capability of the human visual system for brightness discrimination consists of having a subject look at a flat, uniformly illuminated area large enough to occupy the entire field of view. This area typically is a diffuser, such as opaque glass, that is illuminated from behind by a light source whose intensity, I, can be varied. To this field is added an increment of illumination, ΔI, in the form of a short-duration flash that appears as a circle in the center of the uniformly illuminated field, as Fig. 2.5 shows.

If ΔI is not bright enough, the subject says "no," indicating no perceivable change. As ΔI gets stronger, the subject may give a positive response of "yes," indicating a perceived change. Finally, when ΔI is strong enough, the subject will give a response of "yes" all the time. The quantity $\Delta I_c/I$, where ΔI_c is the increment of illumination discriminable 50% of the time with background illumination I, is called the *Weber ratio*. A small value of $\Delta I_c/I$, means that a small percentage change in intensity is discriminable. This represents "good" brightness discrimination. Conversely, a large value of $\Delta I_c/I$, means that a large percentage change in intensity is required. This represents "poor" brightness discrimination.

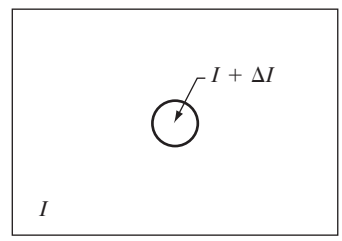

FIGURE 2.5 Basic experimental setup used to characterize brightness discrimination.

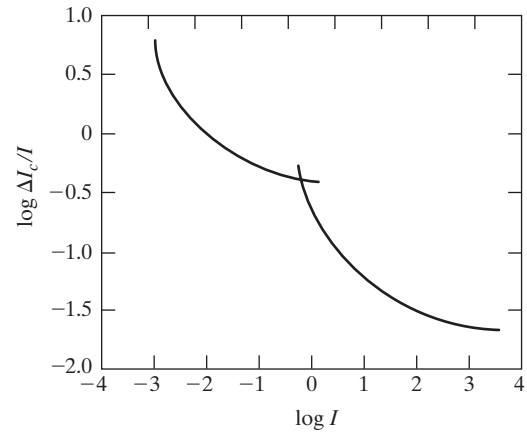

FIGURE 2.6
Typical Weber ratio as a function of intensity.

A plot of $\log \Delta I_c/I$, as a function of $\log I$ has the general shape shown in Fig. 2.6. This curve shows that brightness discrimination is poor (the Weber ratio is large) at low levels of illumination, and it improves significantly (the Weber ratio decreases) as background illumination increases. The two branches in the curve reflect the fact that at low levels of illumination vision is carried out by activity of the rods, whereas at high levels (showing better discrimination) vision is the function of cones.

If the background illumination is held constant and the intensity of the other source, instead of flashing, is now allowed to vary incrementally from never being perceived to always being perceived, the typical observer can discern a total of one to two dozen different intensity changes. Roughly, this result is related to the number of different intensities a person can see at any one point in a monochrome image. This result does not mean that an image can be represented by such a small number of intensity values because, as the eye roams about the image, the average background changes, thus allowing a *different* set of incremental changes to be detected at each new adaptation level. The net consequence is that the eye is capable of a much broader range of *overall* intensity discrimination. In fact, we show in Section 2.4.3 that the eye is capable of detecting objectionable contouring effects in monochrome images whose overall intensity is represented by fewer than approximately two dozen levels.

Two phenomena clearly demonstrate that perceived brightness is not a simple function of intensity. The first is based on the fact that the visual system tends to undershoot or overshoot around the boundary of regions of different intensities. Figure 2.7(a) shows a striking example of this phenomenon. Although the intensity of the stripes is constant, we actually perceive a brightness pattern that is strongly scalloped, especially near the boundaries [Fig. 2.7(b)]. These seemingly scalloped bands are called *Mach bands* after Ernst Mach, who first described the phenomenon in 1865.

The second phenomenon, called *simultaneous contrast*, is related to the fact that a region's perceived brightness does not depend simply on its intensity, as Fig. 2.8 demonstrates. All the center squares have exactly the same intensity.

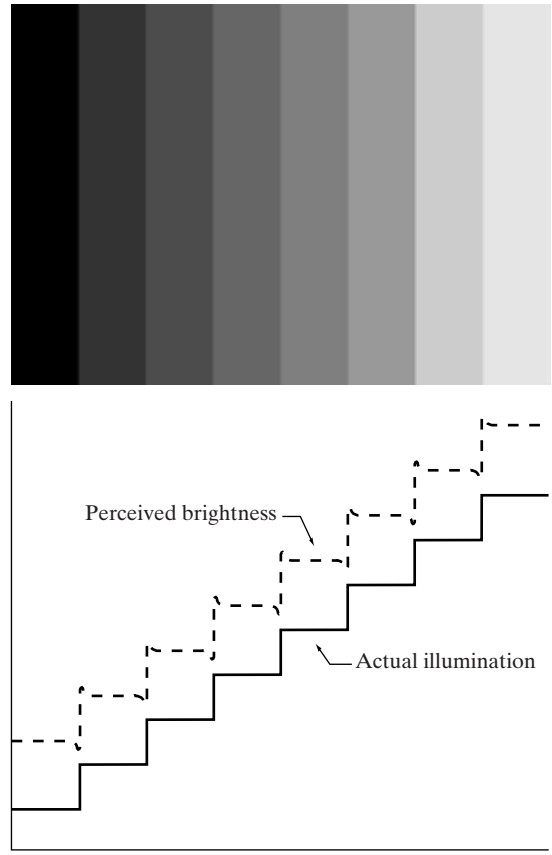

a
b

FIGURE 2.7
(a) An example showing that perceived brightness is not a simple function of intensity. The relative vertical positions between the two profiles in (b) have no special significance; they were chosen for clarity.

However, they appear to the eye to become darker as the background gets lighter. A more familiar example is a piece of paper that seems white when lying on a desk, but can appear totally black when used to shield the eyes while looking directly at a bright sky.

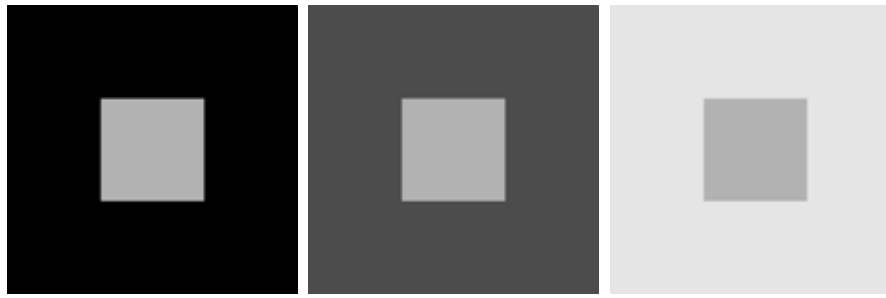

a b c

FIGURE 2.8 Examples of simultaneous contrast. All the inner squares have the same intensity, but they appear progressively darker as the background becomes lighter.

a b
c d

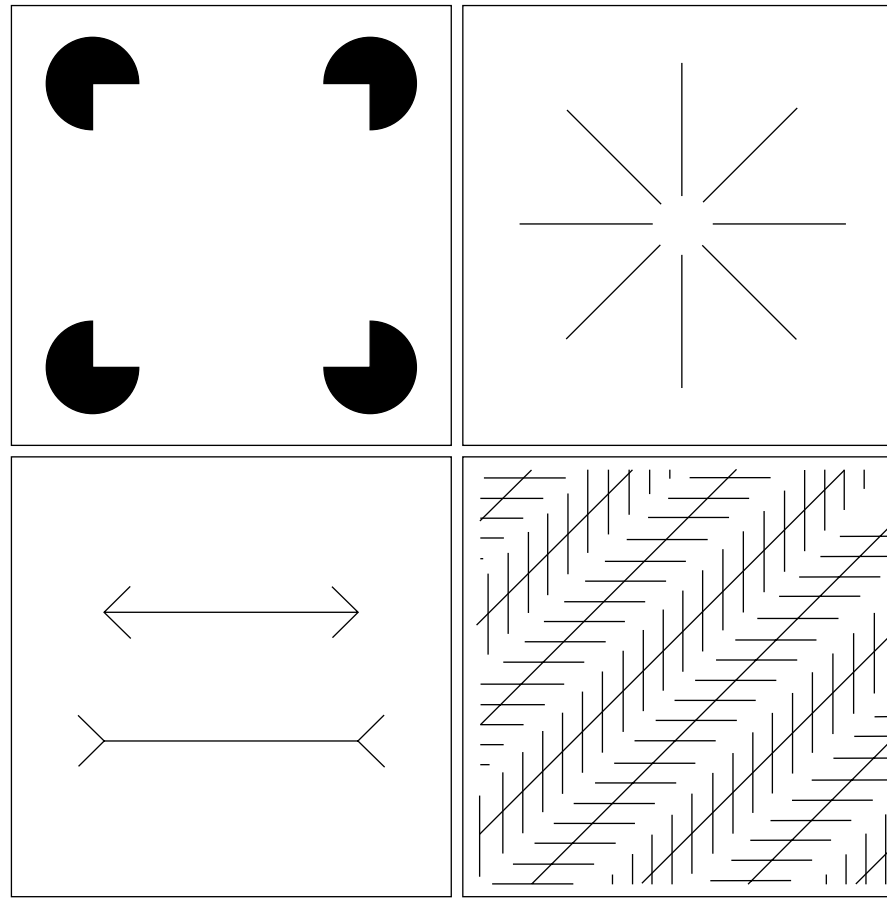

FIGURE 2.9 Some well-known optical illusions.

Other examples of human perception phenomena are optical illusions, in which the eye fills in nonexisting information or wrongly perceives geometrical properties of objects. Some examples are shown in Fig. 2.9. In Fig. 2.9(a), the outline of a square is seen clearly, in spite of the fact that no lines defining such a figure are part of the image. The same effect, this time with a circle, can be seen in Fig. 2.9(b); note how just a few lines are sufficient to give the illusion of a complete circle. The two horizontal line segments in Fig. 2.9(c) are of the same length, but one appears shorter than the other. Finally, all lines in Fig. 2.9(d) that are oriented at 45° are equidistant and parallel. Yet the crosshatching creates the illusion that those lines are far from being parallel. Optical illusions are a characteristic of the human visual system that is not fully understood.

2.2 Light and the Electromagnetic Spectrum

The electromagnetic spectrum was introduced in Section 1.3. We now consider this topic in more detail. In 1666, Sir Isaac Newton discovered that when a beam of sunlight is passed through a glass prism, the emerging beam of light is not

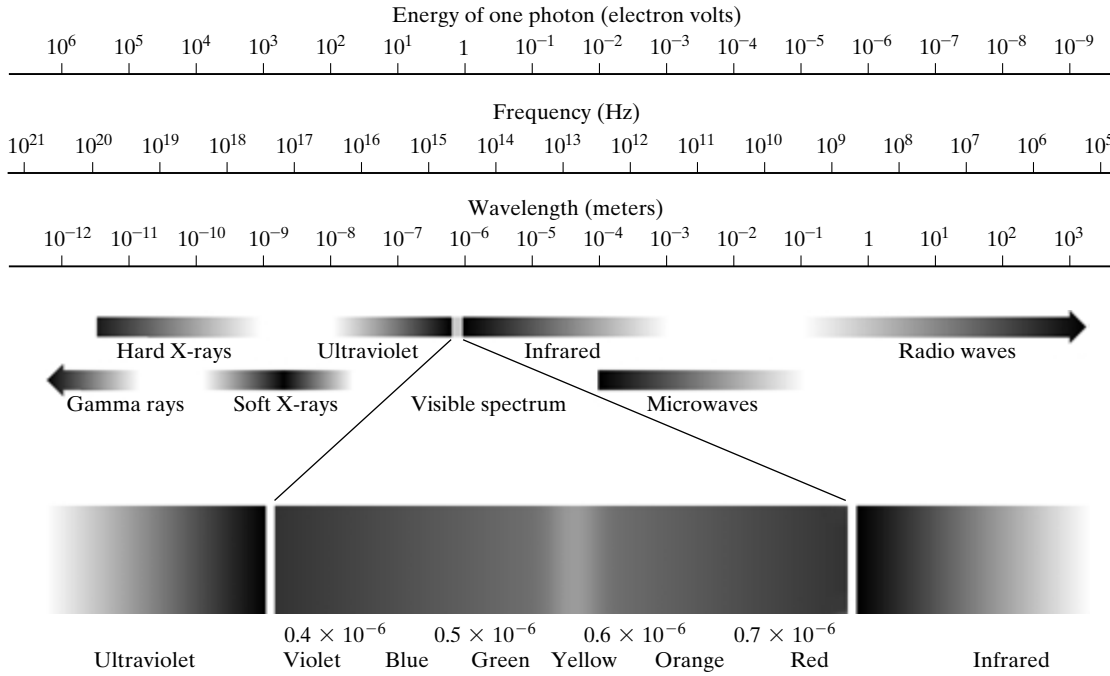

FIGURE 2.10 The electromagnetic spectrum. The visible spectrum is shown zoomed to facilitate explanation, but note that the visible spectrum is a rather narrow portion of the EM spectrum.

white but consists instead of a continuous spectrum of colors ranging from violet at one end to red at the other. As shown in Fig. 2.10, the range of colors we perceive in visible light represents a very small portion of the electromagnetic spectrum. On one end of the spectrum are radio waves with wavelengths billions of times longer than those of visible light. On the other end of the spectrum are gamma rays with wavelengths millions of times smaller than those of visible light. The electromagnetic spectrum can be expressed in terms of wavelength, frequency, or energy. Wavelength (λ) and frequency (ν) are related by the expression

$$\lambda = \frac{c}{\nu} \tag{2.2-1}$$

where c is the speed of light (2.998×10^8 m/s). The energy of the various components of the electromagnetic spectrum is given by the expression

$$E = h\nu \tag{2.2-2}$$

where h is Planck's constant. The units of wavelength are meters, with the terms *microns* (denoted μm and equal to 10^{-6} m) and *nanometers* (10^{-9} m) being used just as frequently. Frequency is measured in Hertz (Hz), with one Hertz being equal to one cycle of a sinusoidal wave per second. A commonly used unit of energy is the electron-volt.

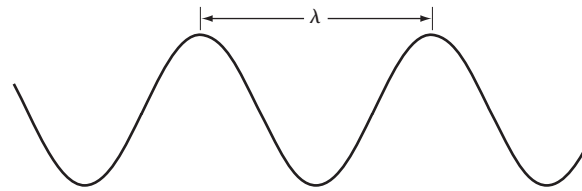

FIGURE 2.11 Graphical representation of one wavelength.

Electromagnetic waves can be visualized as propagating sinusoidal waves with wavelength λ (Fig. 2.11), or they can be thought of as a stream of massless particles, each traveling in a wavelike pattern and moving at the speed of light. Each massless particle contains a certain amount (or bundle) of energy. Each bundle of energy is called a *photon*. We see from Eq. (2.2-2) that energy is proportional to frequency, so the higher-frequency (shorter wavelength) electromagnetic phenomena carry more energy per photon. Thus, radio waves have photons with low energies, microwaves have more energy than radio waves, infrared still more, then visible, ultraviolet, X-rays, and finally gamma rays, the most energetic of all. This is the reason that gamma rays are so dangerous to living organisms.

Light is a particular type of electromagnetic radiation that can be seen and sensed by the human eye. The visible (color) spectrum is shown expanded in Fig. 2.10 for the purpose of discussion (we consider color in much more detail in Chapter 6). The visible band of the electromagnetic spectrum spans the range from approximately 0.43 μm (violet) to about 0.79 μm (red). For convenience, the color spectrum is divided into six broad regions: violet, blue, green, yellow, orange, and red. No color (or other component of the electromagnetic spectrum) ends abruptly, but rather each range blends smoothly into the next, as shown in Fig. 2.10.

The colors that humans perceive in an object are determined by the nature of the light *reflected* from the object. A body that reflects light and is relatively balanced in all visible wavelengths appears white to the observer. However, a body that favors reflectance in a limited range of the visible spectrum exhibits some shades of color. For example, green objects reflect light with wavelengths primarily in the 500 to 570 nm range while absorbing most of the energy at other wavelengths.

Light that is void of color is called *achromatic* or *monochromatic* light. The only attribute of such light is its *intensity*, or amount. The term *gray level* generally is used to describe monochromatic intensity because it ranges from black, to grays, and finally to white. Chromatic light spans the electromagnetic energy spectrum from approximately 0.43 to 0.79 μm, as noted previously. Three basic quantities are used to describe the quality of a chromatic light source: radiance; luminance; and brightness. *Radiance* is the total amount of energy that flows from the light source, and it is usually measured in watts (W). *Luminance*, measured in lumens (lm), gives a measure of the amount of energy an observer *perceives* from a light source. For example, light emitted from a source operating in the far infrared region of the spectrum could have significant energy (radiance), but an observer would hardly perceive it; its luminance would be almost zero. Finally, as discussed in Section 2.1, *brightness* is a subjective descriptor of light perception that is practically impossible to measure. It embod-

ies the achromatic notion of intensity and is one of the key factors in describing color sensation.

Continuing with the discussion of Fig. 2.10, we note that at the short-wavelength end of the electromagnetic spectrum, we have gamma rays and hard X-rays. As discussed in Section 1.3.1, gamma radiation is important for medical and astronomical imaging, and for imaging radiation in nuclear environments. Hard (high-energy) X-rays are used in industrial applications. Chest X-rays are in the high end (shorter wavelength) of the soft X-rays region and dental X-rays are in the lower energy end of that band. The soft X-ray band transitions into the far ultraviolet light region, which in turn blends with the visible spectrum at longer wavelengths. Moving still higher in wavelength, we encounter the infrared band, which radiates heat, a fact that makes it useful in imaging applications that rely on "heat signatures." The part of the infrared band close to the visible spectrum is called the *near-infrared* region. The opposite end of this band is called the *far-infrared* region. This latter region blends with the microwave band. This band is well known as the source of energy in microwave ovens, but it has many other uses, including communication and radar. Finally, the radio wave band encompasses television as well as AM and FM radio. In the higher energies, radio signals emanating from certain stellar bodies are useful in astronomical observations. Examples of images in most of the bands just discussed are given in Section 1.3.

In principle, if a sensor can be developed that is capable of detecting energy radiated by a band of the electromagnetic spectrum, we can image events of interest in that band. It is important to note, however, that the wavelength of an electromagnetic wave required to "see" an object must be of the same size as or smaller than the object. For example, a water molecule has a diameter on the order of 10^{-10} m. Thus, to study molecules, we would need a source capable of emitting in the far ultraviolet or soft X-ray region. This limitation, along with the physical properties of the sensor material, establishes the fundamental limits on the capability of imaging sensors, such as visible, infrared, and other sensors in use today.

Although imaging is based predominantly on energy radiated by electromagnetic waves, this is not the only method for image generation. For example, as discussed in Section 1.3.7, sound reflected from objects can be used to form ultrasonic images. Other major sources of digital images are electron beams for electron microscopy and synthetic images used in graphics and visualization.

2.3 Image Sensing and Acquisition

The types of images in which we are interested are generated by the combination of an "illumination" source and the reflection or absorption of energy from that source by the elements of the "scene" being imaged. We enclose *illumination* and *scene* in quotes to emphasize the fact that they are considerably more general than the familiar situation in which a visible light source illuminates a common everyday 3-D (three-dimensional) scene. For example, the illumination may originate from a source of electromagnetic energy such as radar, infrared,

or X-ray energy. But, as noted earlier, it could originate from less traditional sources, such as ultrasound or even a computer-generated illumination pattern. Similarly, the scene elements could be familiar objects, but they can just as easily be molecules, buried rock formations, or a human brain. We could even image a source, such as acquiring images of the sun. Depending on the nature of the source, illumination energy is reflected from, or transmitted through, objects. An example in the first category is light reflected from a planar surface. An example in the second category is when X-rays pass through a patient's body for the purpose of generating a diagnostic X-ray film. In some applications, the reflected or transmitted energy is focused onto a photoconverter (e.g., a phosphor screen), which converts the energy into visible light. Electron microscopy and some applications of gamma imaging use this approach.

Figure 2.12 shows the three principal sensor arrangements used to transform illumination energy into digital images. The idea is simple: Incoming energy is

a
b
c

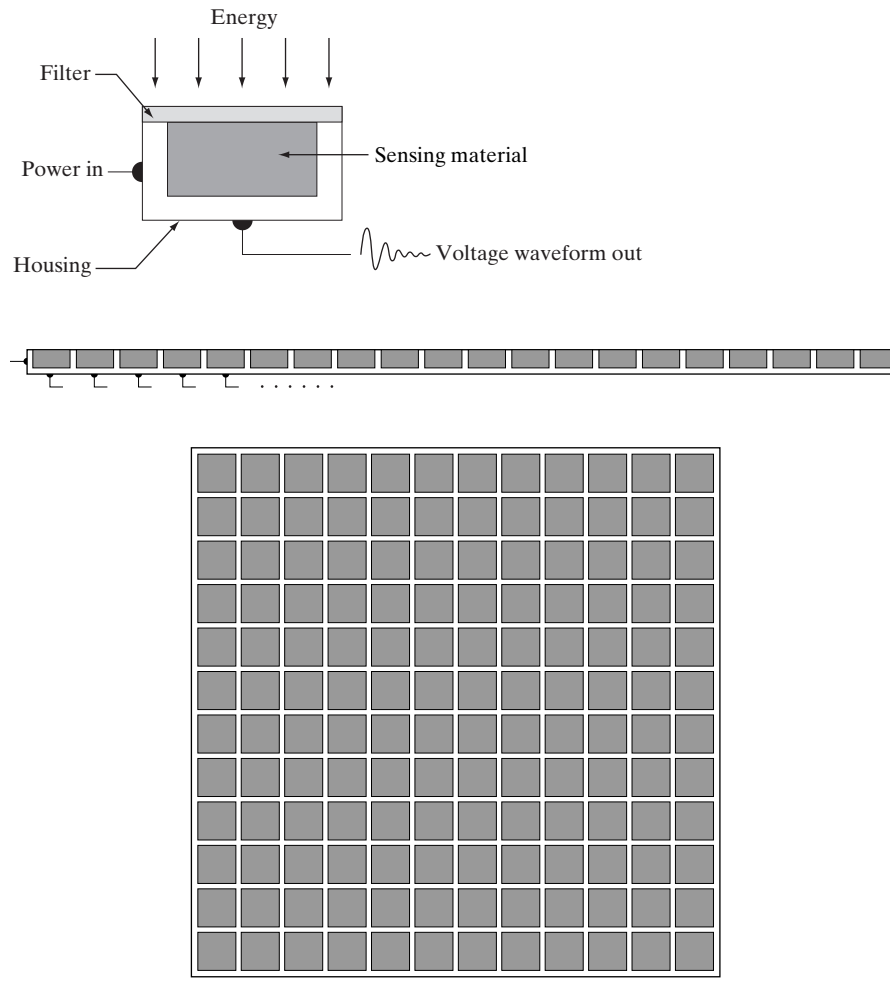

FIGURE 2.12
(a) Single imaging sensor.
(b) Line sensor.
(c) Array sensor.

transformed into a voltage by the combination of input electrical power and sensor material that is responsive to the particular type of energy being detected. The output voltage waveform is the response of the sensor(s), and a digital quantity is obtained from each sensor by digitizing its response. In this section, we look at the principal modalities for image sensing and generation. Image digitizing is discussed in Section 2.4.

2.3.1 Image Acquisition Using a Single Sensor

Figure 2.12(a) shows the components of a single sensor. Perhaps the most familiar sensor of this type is the photodiode, which is constructed of silicon materials and whose output voltage waveform is proportional to light. The use of a filter in front of a sensor improves selectivity. For example, a green (pass) filter in front of a light sensor favors light in the green band of the color spectrum. As a consequence, the sensor output will be stronger for green light than for other components in the visible spectrum.

In order to generate a 2-D image using a single sensor, there has to be relative displacements in both the x- and y-directions between the sensor and the area to be imaged. Figure 2.13 shows an arrangement used in high-precision scanning, where a film negative is mounted onto a drum whose mechanical rotation provides displacement in one dimension. The single sensor is mounted on a lead screw that provides motion in the perpendicular direction. Since mechanical motion can be controlled with high precision, this method is an inexpensive (but slow) way to obtain high-resolution images. Other similar mechanical arrangements use a flat bed, with the sensor moving in two linear directions. These types of mechanical digitizers sometimes are referred to as *microdensitometers*.

Another example of imaging with a single sensor places a laser source coincident with the sensor. Moving mirrors are used to control the outgoing beam in a scanning pattern and to direct the reflected laser signal onto the sensor. This arrangement also can be used to acquire images using strip and array sensors, which are discussed in the following two sections.

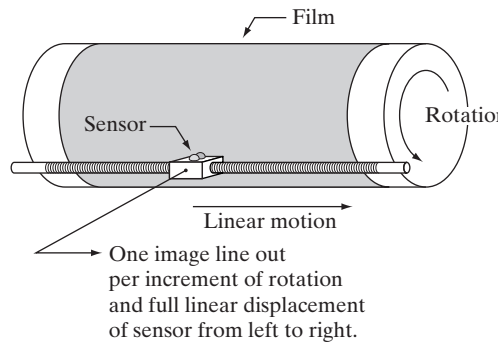

FIGURE 2.13 Combining a single sensor with motion to generate a 2-D image.

2.3.2 Image Acquisition Using Sensor Strips

A geometry that is used much more frequently than single sensors consists of an in-line arrangement of sensors in the form of a sensor strip, as Fig. 2.12(b) shows. The strip provides imaging elements in one direction. Motion perpendicular to the strip provides imaging in the other direction, as shown in Fig. 2.14(a). This is the type of arrangement used in most flat bed scanners. Sensing devices with 4000 or more in-line sensors are possible. In-line sensors are used routinely in airborne imaging applications, in which the imaging system is mounted on an aircraft that flies at a constant altitude and speed over the geographical area to be imaged. One-dimensional imaging sensor strips that respond to various bands of the electromagnetic spectrum are mounted perpendicular to the direction of flight. The imaging strip gives one line of an image at a time, and the motion of the strip completes the other dimension of a two-dimensional image. Lenses or other focusing schemes are used to project the area to be scanned onto the sensors.

Sensor strips mounted in a ring configuration are used in medical and industrial imaging to obtain cross-sectional ("slice") images of 3-D objects, as Fig. 2.14(b) shows. A rotating X-ray source provides illumination and the por-

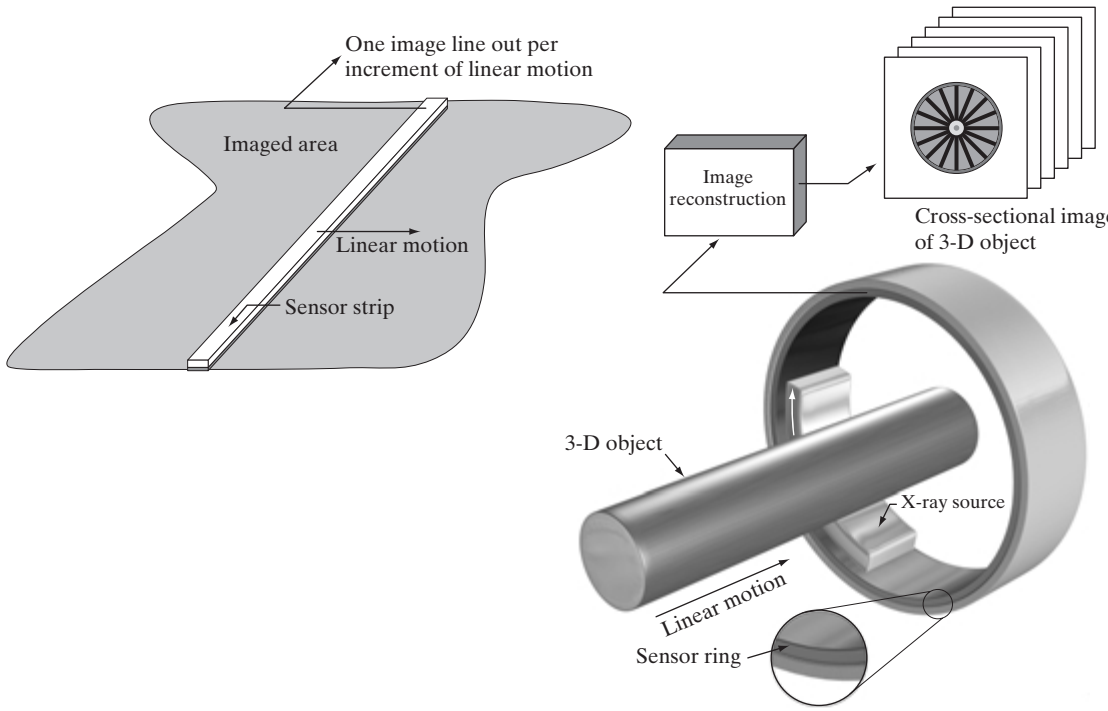

a b

FIGURE 2.14 (a) Image acquisition using a linear sensor strip. (b) Image acquisition using a circular sensor strip.

tion of the sensors opposite the source collect the X-ray energy that pass through the object (the sensors obviously have to be sensitive to X-ray energy). This is the basis for medical and industrial computerized axial tomography (CAT) imaging as indicated in Sections 1.2 and 1.3.2. It is important to note that the output of the sensors must be processed by reconstruction algorithms whose objective is to transform the sensed data into meaningful cross-sectional images. In other words, images are not obtained directly from the sensors by motion alone; they require extensive processing. A 3-D digital volume consisting of stacked images is generated as the object is moved in a direction perpendicular to the sensor ring. Other modalities of imaging based on the CAT principle include magnetic resonance imaging (MRI) and positron emission tomography (PET). The illumination sources, sensors, and types of images are different, but conceptually they are very similar to the basic imaging approach shown in Fig. 2.14(b).

2.3.3 Image Acquisition Using Sensor Arrays

Figure 2.12(c) shows individual sensors arranged in the form of a 2-D array. Numerous electromagnetic and some ultrasonic sensing devices frequently are arranged in an array format. This is also the predominant arrangement found in digital cameras. A typical sensor for these cameras is a CCD array, which can be manufactured with a broad range of sensing properties and can be packaged in rugged arrays of 4000×4000 elements or more. CCD sensors are used widely in digital cameras and other light sensing instruments. The response of each sensor is proportional to the integral of the light energy projected onto the surface of the sensor, a property that is used in astronomical and other applications requiring low noise images. Noise reduction is achieved by letting the sensor integrate the input light signal over minutes or even hours (we discuss noise reduction by integration in Chapter 3). Since the sensor array shown in Fig. 2.15(c) is two dimensional, its key advantage is that a complete image can be obtained by focusing the energy pattern onto the surface of the array. Motion obviously is not necessary, as is the case with the sensor arrangements discussed in the preceding two sections.

The principal manner in which array sensors are used is shown in Fig. 2.15. This figure shows the energy from an illumination source being reflected from a scene element, but, as mentioned at the beginning of this section, the energy also could be transmitted through the scene elements. The first function performed by the imaging system shown in Fig. 2.15(c) is to collect the incoming energy and focus it onto an image plane. If the illumination is light, the front end of the imaging system is a lens, which projects the viewed scene onto the lens focal plane, as Fig. 2.15(d) shows. The sensor array, which is coincident with the focal plane, produces outputs proportional to the integral of the light received at each sensor. Digital and analog circuitry sweep these outputs and convert them to a video signal, which is then digitized by another section of the imaging system. The output is a digital image, as shown diagrammatically in Fig. 2.15(e). Conversion of an image into digital form is the topic of Section 2.4.

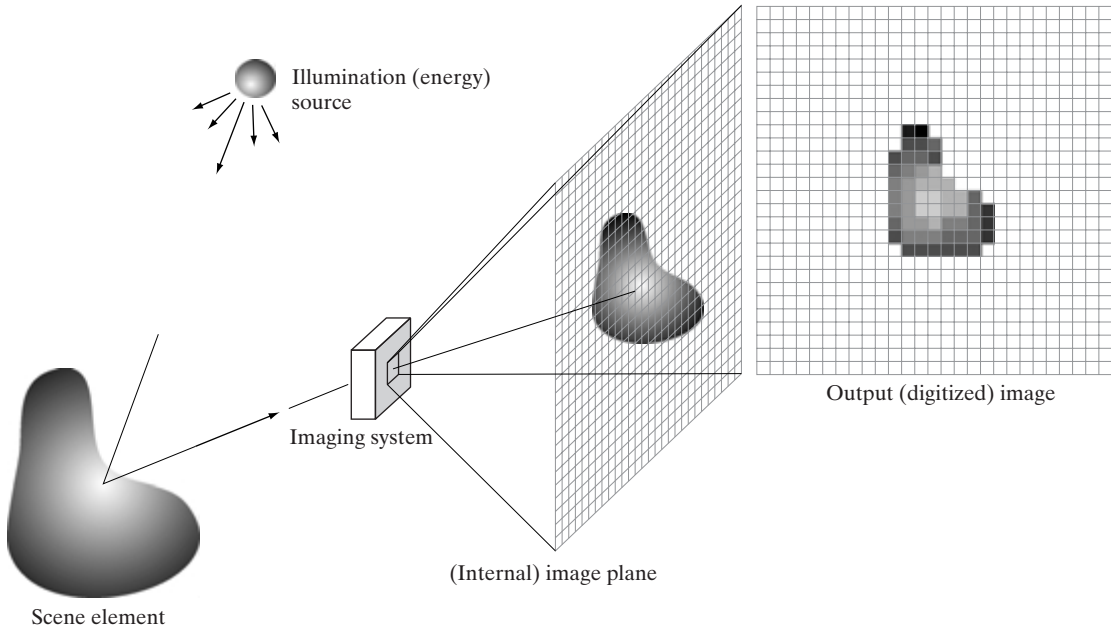

a
b c d e

FIGURE 2.15 An example of the digital image acquisition process. (a) Energy ("illumination") source. (b) An element of a scene. (c) Imaging system. (d) Projection of the scene onto the image plane. (e) Digitized image.

2.3.4 A Simple Image Formation Model

As introduced in Section 1.1, we shall denote images by two-dimensional functions of the form $f(x, y)$. The value or amplitude of f at spatial coordinates (x, y) is a positive scalar quantity whose physical meaning is determined by the source of the image. Most of the images in which we are interested in this book are monochromatic images, whose values are said to span the gray scale, as discussed in Section 2.2. When an image is generated from a physical process, its values are proportional to energy radiated by a physical source (e.g., electromagnetic waves). As a consequence, $f(x, y)$ must be nonzero and finite; that is,

$$0 < f(x, y) < \infty. \tag{2.3-1}$$

The function $f(x, y)$ may be characterized by two components: (1) the amount of source illumination incident on the scene being viewed, and (2) the amount of illumination reflected by the objects in the scene. Appropriately, these are called the *illumination* and *reflectance* components and are denoted by $i(x, y)$ and $r(x, y)$, respectively. The two functions combine as a product to form $f(x, y)$:

$$f(x, y) = i(x, y)r(x, y) \tag{2.3-2}$$

where

$$0 < i(x, y) < \infty \tag{2.3-3}$$

and

$$0 < r(x, y) < 1. \tag{2.3-4}$$

Equation (2.3-4) indicates that reflectance is bounded by 0 (total absorption) and 1 (total reflectance). The nature of $i(x, y)$ is determined by the illumination source, and $r(x, y)$ is determined by the characteristics of the imaged objects. It is noted that these expressions also are applicable to images formed via transmission of the illumination through a medium, such as a chest X-ray. In this case, we would deal with a *transmissivity* instead of a *reflectivity* function, but the limits would be the same as in Eq. (2.3-4), and the image function formed would be modeled as the product in Eq. (2.3-2).

EXAMPLE 2.1: Some typical values of illumination and reflectance.

■ The values given in Eqs. (2.3-3) and (2.3-4) are theoretical bounds. The following *average* numerical figures illustrate some typical ranges of $i(x, y)$ for visible light. On a clear day, the sun may produce in excess of 90,000 lm/m^2 of illumination on the surface of the Earth. This figure decreases to less than 10,000 lm/m^2 on a cloudy day. On a clear evening, a full moon yields about 0.1 lm/m^2 of illumination. The typical illumination level in a commercial office is about 1000 lm/m^2. Similarly, the following are some typical values of $r(x, y)$: 0.01 for black velvet, 0.65 for stainless steel, 0.80 for flat-white wall paint, 0.90 for silver-plated metal, and 0.93 for snow. ■

As noted in Section 2.2, we call the intensity of a monochrome image at any coordinates (x_0, y_0) the *gray level* (ℓ) of the image at that point. That is,

$$\ell = f(x_0, y_0) \tag{2.3-5}$$

From Eqs. (2.3-2) through (2.3-4), it is evident that ℓ lies in the range

$$L_{\min} \leq \ell \leq L_{\max} \tag{2.3-6}$$

In theory, the only requirement on $L_{\min}$ is that it be positive, and on $L_{\max}$ that it be finite. In practice, $L_{\min} = i_{\min}r_{\min}$ and $L_{\max} = i_{\max}r_{\max}$. Using the preceding average office illumination and range of reflectance values as guidelines, we may expect $L_{\min} \approx 10$ and $L_{\max} \approx 1000$ to be typical limits for indoor values in the absence of additional illumination.

The interval $[L_{\min}, L_{\max}]$ is called the *gray scale*. Common practice is to shift this interval numerically to the interval $[0, L - 1]$, where $\ell = 0$ is considered black and $\ell = L - 1$ is considered white on the gray scale. All intermediate values are shades of gray varying from black to white.

2.4 Image Sampling and Quantization

From the discussion in the preceding section, we see that there are numerous ways to acquire images, but our objective in all is the same: to generate digital images from sensed data. The output of most sensors is a continuous voltage waveform whose amplitude and spatial behavior are related to the physical phenomenon being sensed. To create a digital image, we need to convert the continuous sensed data into digital form. This involves two processes: *sampling* and *quantization*.

2.4.1 Basic Concepts in Sampling and Quantization

The basic idea behind sampling and quantization is illustrated in Fig. 2.16. Figure 2.16(a) shows a continuous image, $f(x, y)$, that we want to convert to digital form. An image may be continuous with respect to the x- and y-coordinates, and also in amplitude. To convert it to digital form, we have to sample the function in both coordinates and in amplitude. Digitizing the coordinate values is called *sampling*. Digitizing the amplitude values is called *quantization*.

The one-dimensional function shown in Fig. 2.16(b) is a plot of amplitude (gray level) values of the continuous image along the line segment AB in Fig. 2.16(a). The random variations are due to image noise. To sample this function, we take equally spaced samples along line AB, as shown in Fig. 2.16(c). The location of each sample is given by a vertical tick mark in the bottom part of the figure. The samples are shown as small white squares superimposed on the function. The set of these discrete locations gives the sampled function. However, the values of the samples still span (vertically) a continuous range of gray-level values. In order to form a digital function, the gray-level values also must be converted (*quantized*) into discrete quantities. The right side of Fig. 2.16(c) shows the gray-level scale divided into eight discrete levels, ranging from black to white. The vertical tick marks indicate the specific value assigned to each of the eight gray levels. The continuous gray levels are quantized simply by assigning one of the eight discrete gray levels to each sample. The assignment is made depending on the vertical proximity of a sample to a vertical tick mark. The digital samples resulting from both sampling and quantization are shown in Fig. 2.16(d). Starting at the top of the image and carrying out this procedure line by line produces a two-dimensional digital image.

Sampling in the manner just described assumes that we have a continuous image in both coordinate directions as well as in amplitude. In practice, the method of sampling is determined by the sensor arrangement used to generate the image. When an image is generated by a single sensing element combined with mechanical motion, as in Fig. 2.13, the output of the sensor is quantized in the manner described above. However, sampling is accomplished by selecting the number of individual mechanical increments at which we activate the sensor to collect data. Mechanical motion can be made very exact so, in principle, there is almost no limit as to how fine we can sample an image. However, practical limits are established by imperfections in the optics used to focus on the

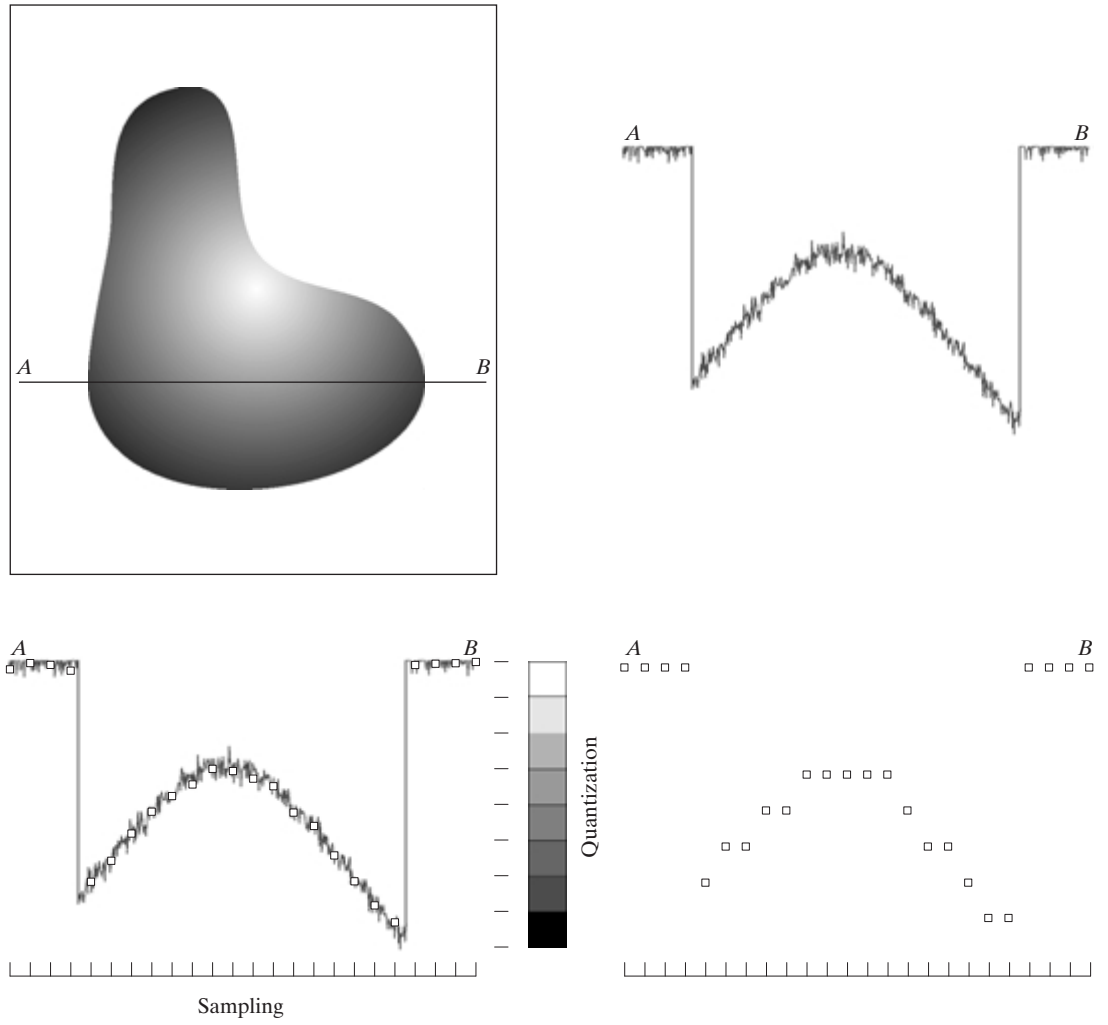

a b
c d

FIGURE 2.16 Generating a digital image. (a) Continuous image. (b) A scan line from *A* to *B* in the continuous image, used to illustrate the concepts of sampling and quantization. (c) Sampling and quantization. (d) Digital scan line.

sensor an illumination spot that is inconsistent with the fine resolution achievable with mechanical displacements.

When a sensing strip is used for image acquisition, the number of sensors in the strip establishes the sampling limitations in one image direction. Mechanical motion in the other direction can be controlled more accurately, but it makes little sense to try to achieve sampling density in one direction that exceeds the

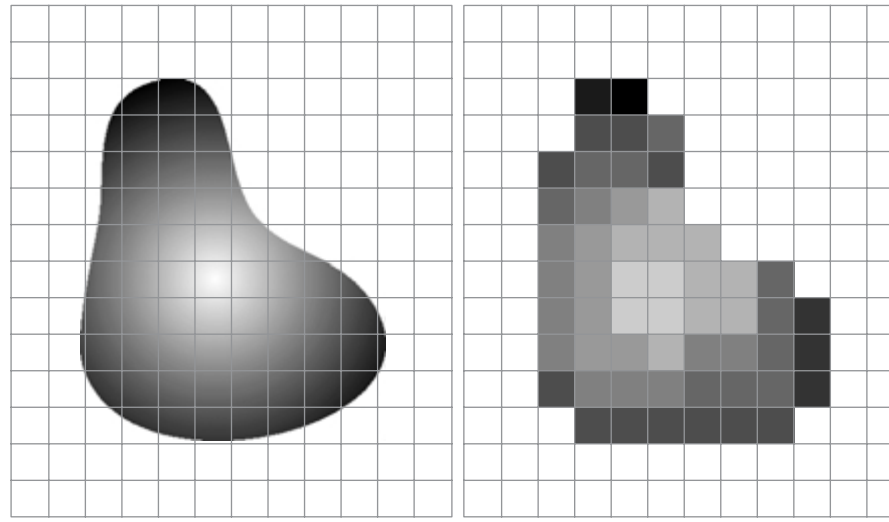

a b

FIGURE 2.17 (a) Continuos image projected onto a sensor array. (b) Result of image sampling and quantization.

sampling limits established by the number of sensors in the other. Quantization of the sensor outputs completes the process of generating a digital image.

When a sensing array is used for image acquisition, there is no motion and the number of sensors in the array establishes the limits of sampling in both directions. Quantization of the sensor outputs is as before. Figure 2.17 illustrates this concept. Figure 2.17(a) shows a continuous image projected onto the plane of an array sensor. Figure 2.17(b) shows the image after sampling and quantization. Clearly, the quality of a digital image is determined to a large degree by the number of samples and discrete gray levels used in sampling and quantization. However, as shown in Section 2.4.3, image content is an important consideration in choosing these parameters.

2.4.2 Representing Digital Images

The result of sampling and quantization is a matrix of real numbers. We will use two principal ways in this book to represent digital images. Assume that an image $f(x, y)$ is sampled so that the resulting digital image has M rows and N columns. The values of the coordinates (x, y) now become *discrete* quantities. For notational clarity and convenience, we shall use integer values for these discrete coordinates. Thus, the values of the coordinates at the origin are $(x, y) = (0, 0)$. The next coordinate values along the first row of the image are represented as $(x, y) = (0, 1)$. It is important to keep in mind that the notation $(0, 1)$ is used to signify the second sample along the first row. It does *not* mean that these are the actual values of physical coordinates when the image was sampled. Figure 2.18 shows the coordinate convention used throughout this book.

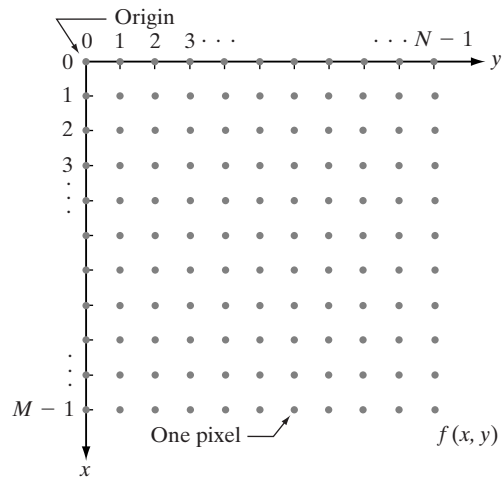

FIGURE 2.18 Coordinate convention used in this book to represent digital images.

The notation introduced in the preceding paragraph allows us to write the complete $M \times N$ digital image in the following compact matrix form:

$$f(x, y) = \begin{bmatrix} f(0,0) & f(0,1) & \cdots & f(0, N-1) \\ f(1,0) & f(1,1) & \cdots & f(1, N-1) \\ \vdots & \vdots & & \vdots \\ f(M-1,0) & f(M-1,1) & \cdots & f(M-1, N-1) \end{bmatrix}. \quad (2.4\text{-}1)$$

The right side of this equation is by definition a digital image. Each element of this matrix array is called an *image element*, *picture element*, *pixel*, or *pel*. The terms *image* and *pixel* will be used throughout the rest of our discussions to denote a digital image and its elements.

In some discussions, it is advantageous to use a more traditional matrix notation to denote a digital image and its elements:

$$\mathbf{A} = \begin{bmatrix} a_{0,0} & a_{0,1} & \cdots & a_{0,N-1} \\ a_{1,0} & a_{1,1} & \cdots & a_{1,N-1} \\ \vdots & \vdots & & \vdots \\ a_{M-1,0} & a_{M-1,1} & \cdots & a_{M-1,N-1} \end{bmatrix}. \quad (2.4\text{-}2)$$

Clearly, $a_{ij} = f(x = i, y = j) = f(i, j)$, so Eqs. (2.4-1) and (2.4-2) are identical matrices.

Expressing sampling and quantization in more formal mathematical terms can be useful at times. Let Z and R denote the set of real integers and the set of real numbers, respectively. The sampling process may be viewed as partitioning the xy plane into a grid, with the coordinates of the center of each grid being a pair of elements from the Cartesian product Z^2, which is the set of all ordered pairs of elements (z_i, z_j), with z_i and z_j being integers from Z. Hence, $f(x, y)$ is a digital image if (x, y) are integers from Z^2 and f is a function that assigns a gray-level value (that is, a real number from the set of real numbers, R) to each distinct pair of coordinates (x, y). This functional assignment

obviously is the quantization process described earlier. If the gray levels also are integers (as usually is the case in this and subsequent chapters), Z replaces R, and a digital image then becomes a 2-D function whose coordinates and amplitude values are integers.

This digitization process requires decisions about values for M, N, and for the number, L, of discrete gray levels allowed for each pixel. There are no requirements on M and N, other than that they have to be positive integers. However, due to processing, storage, and sampling hardware considerations, the number of gray levels typically is an integer power of 2:

$$L = 2^k. \tag{2.4-3}$$

We assume that the discrete levels are equally spaced and that they are integers in the interval $[0, L - 1]$. Sometimes the range of values spanned by the gray scale is called the *dynamic range* of an image, and we refer to images whose gray levels span a significant portion of the gray scale as having a high dynamic range. When an appreciable number of pixels exhibit this property, the image will have high contrast. Conversely, an image with low dynamic range tends to have a dull, washed out gray look. This is discussed in much more detail in Section 3.3.

The number, b, of bits required to store a digitized image is

$$b = M \times N \times k. \tag{2.4-4}$$

When $M = N$, this equation becomes

$$b = N^2 k. \tag{2.4-5}$$

Table 2.1 shows the number of bits required to store square images with various values of N and k. The number of gray levels corresponding to each value of k is shown in parentheses. When an image can have 2^k gray levels, it is common practice to refer to the image as a "k-bit image." For example, an image with 256 possible gray-level values is called an 8-bit image. Note that storage requirements for 8-bit images of size 1024×1024 and higher are not insignificant.

TABLE 2.1
Number of storage bits for various values of N and k.

N/k	1 ($L = 2$)	2 ($L = 4$)	3 ($L = 8$)	4 ($L = 16$)	5 ($L = 32$)	6 ($L = 64$)	7 ($L = 128$)	8 ($L = 256$)
32	1,024	2,048	3,072	4,096	5,120	6,144	7,168	8,192
64	4,096	8,192	12,288	16,384	20,480	24,576	28,672	32,768
128	16,384	32,768	49,152	65,536	81,920	98,304	114,688	131,072
256	65,536	131,072	196,608	262,144	327,680	393,216	458,752	524,288
512	262,144	524,288	786,432	1,048,576	1,310,720	1,572,864	1,835,008	2,097,152
1024	1,048,576	2,097,152	3,145,728	4,194,304	5,242,880	6,291,456	7,340,032	8,388,608
2048	4,194,304	8,388,608	12,582,912	16,777,216	20,971,520	25,165,824	29,369,128	33,554,432
4096	16,777,216	33,554,432	50,331,648	67,108,864	83,886,080	100,663,296	117,440,512	134,217,728
8192	67,108,864	134,217,728	201,326,592	268,435,456	335,544,320	402,653,184	469,762,048	536,870,912

2.4.3 Spatial and Gray-Level Resolution

Sampling is the principal factor determining the *spatial resolution* of an image. Basically, spatial resolution is the smallest discernible detail in an image. Suppose that we construct a chart with vertical lines of width W, with the space between the lines also having width W. A *line pair* consists of one such line and its adjacent space. Thus, the width of a line pair is $2W$, and there are $1/2W$ line pairs per unit distance. A widely used definition of resolution is simply the smallest number of discernible line pairs per unit distance; for example, 100 line pairs per millimeter.

Gray-level resolution similarly refers to the smallest discernible change in gray level, but, as noted in Section 2.1.3, measuring discernible changes in gray level is a highly subjective process. We have considerable discretion regarding the number of samples used to generate a digital image, but this is not true for the number of gray levels. Due to hardware considerations, the number of gray levels is usually an integer power of 2, as mentioned in the previous section. The most common number is 8 bits, with 16 bits being used in some applications where enhancement of specific gray-level ranges is necessary. Sometimes we find systems that can digitize the gray levels of an image with 10 or 12 bits of accuracy, but these are the exception rather than the rule.

When an actual measure of physical resolution relating pixels and the level of detail they resolve in the original scene are not necessary, it is not uncommon to refer to an L-level digital image of size $M \times N$ as having a spatial resolution of $M \times N$ pixels and a gray-level resolution of L levels. We will use this terminology from time to time in subsequent discussions, making a reference to actual resolvable detail only when necessary for clarity.

EXAMPLE 2.2: Typical effects of varying the number of samples in a digital image.

■ Figure 2.19 shows an image of size 1024×1024 pixels whose gray levels are represented by 8 bits. The other images shown in Fig. 2.19 are the results of

FIGURE 2.19 A 1024×1024, 8-bit image subsampled down to size 32×32 pixels. The number of allowable gray levels was kept at 256.

subsampling the 1024 × 1024 image. The subsampling was accomplished by deleting the appropriate number of rows and columns from the original image. For example, the 512 × 512 image was obtained by deleting every other row and column from the 1024 × 1024 image. The 256 × 256 image was generated by deleting every other row and column in the 512 × 512 image, and so on. The number of allowed gray levels was kept at 256.

These images show the dimensional proportions between various sampling densities, but their size differences make it difficult to see the effects resulting from a reduction in the number of samples. The simplest way to compare these effects is to bring all the subsampled images up to size 1024 × 1024 by row and column pixel replication. The results are shown in Figs. 2.20(b) through (f). Figure 2.20(a) is the same 1024 × 1024, 256-level image shown in Fig. 2.19; it is repeated to facilitate comparisons.

Compare Fig. 2.20(a) with the 512 × 512 image in Fig. 2.20(b) and note that it is virtually impossible to tell these two images apart. The level of detail lost is simply too fine to be seen on the printed page at the scale in which these im-

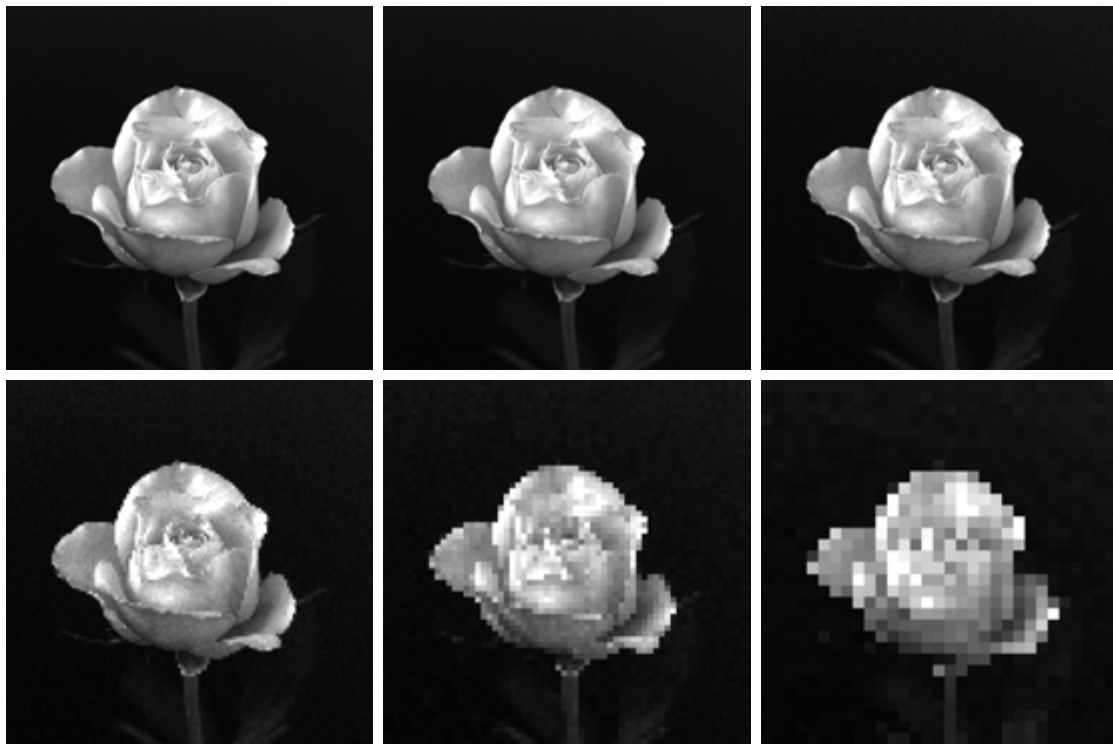

a b c
d e f

FIGURE 2.20 (a) 1024 × 1024, 8-bit image. (b) 512 × 512 image resampled into 1024 × 1024 pixels by row and column duplication. (c) through (f) 256 × 256, 128 × 128, 64 × 64, and 32 × 32 images resampled into 1024 × 1024 pixels.

ages are shown. Next, the 256 × 256 image in Fig. 2.20(c) shows a very slight fine checkerboard pattern in the borders between flower petals and the black background. A slightly more pronounced graininess throughout the image also is beginning to appear. These effects are much more visible in the 128 × 128 image in Fig. 2.20(d), and they become pronounced in the 64 × 64 and 32 × 32 images in Figs. 2.20(e) and (f), respectively. ■

EXAMPLE 2.3: Typical effects of varying the number of gray levels in a digital image.

■ In this example, we keep the number of samples constant and reduce the number of gray levels from 256 to 2, in integer powers of 2. Figure 2.21(a) is a 452 × 374 CAT projection image, displayed with $k = 8$ (256 gray levels). Images such as this are obtained by fixing the X-ray source in one position, thus producing a 2-D image

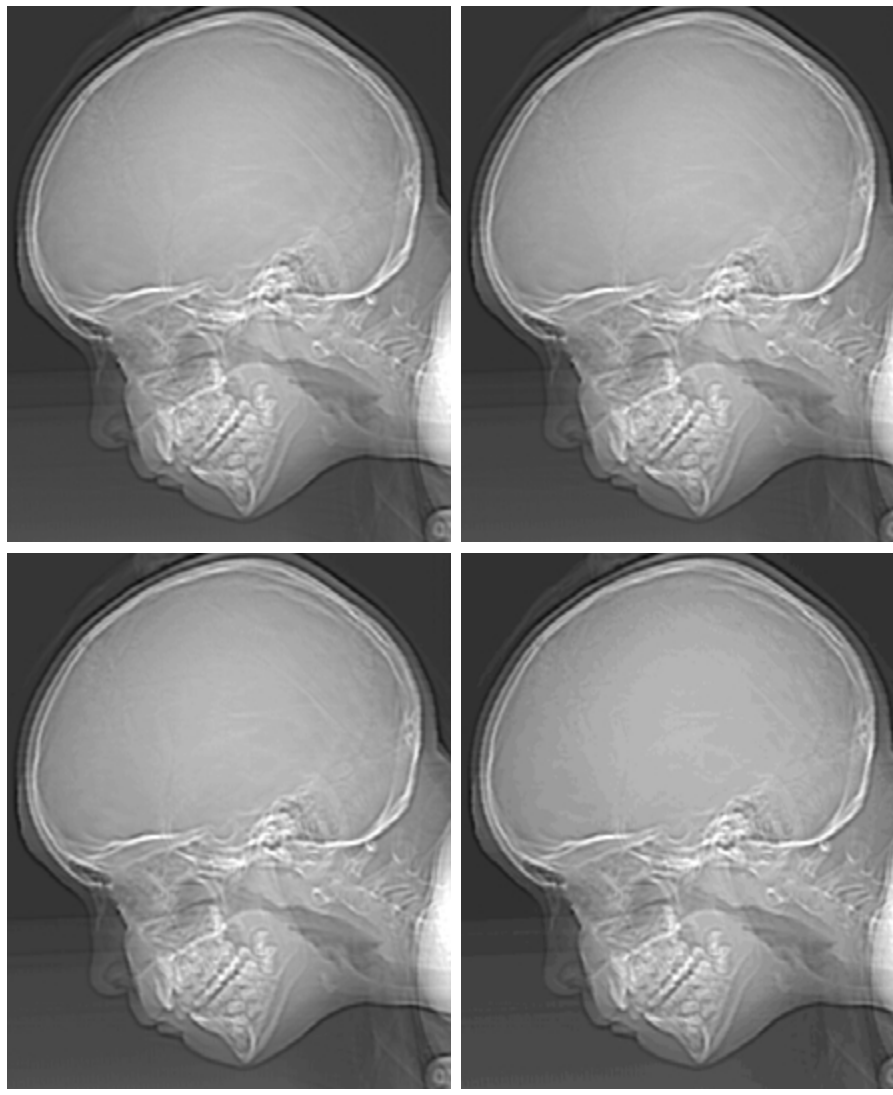

a b
c d

FIGURE 2.21 (a) 452 × 374, 256-level image. (b)–(d) Image displayed in 128, 64, and 32 gray levels, while keeping the spatial resolution constant.

in any desired direction. Projection images are used as guides to set up the parameters for a CAT scanner, including tilt, number of slices, and range.

Figures 2.21(b) through (h) were obtained by reducing the number of bits from $k = 7$ to $k = 1$ while keeping the spatial resolution constant at 452×374 pixels. The 256-, 128-, and 64-level images are visually identical for all practical purposes. The 32-level image shown in Fig. 2.21(d), however, has an almost imperceptible set of very fine ridgelike structures in areas of smooth gray levels (particularly in the skull). This effect, caused by the use of an insufficient number of gray levels in smooth areas of a digital image, is called *false contouring*, so called because the ridges resemble topographic contours in a map. False contouring generally is quite visible in images displayed using 16 or less uniformly spaced gray levels, as the images in Figs. 2.21(e) through (h) show.

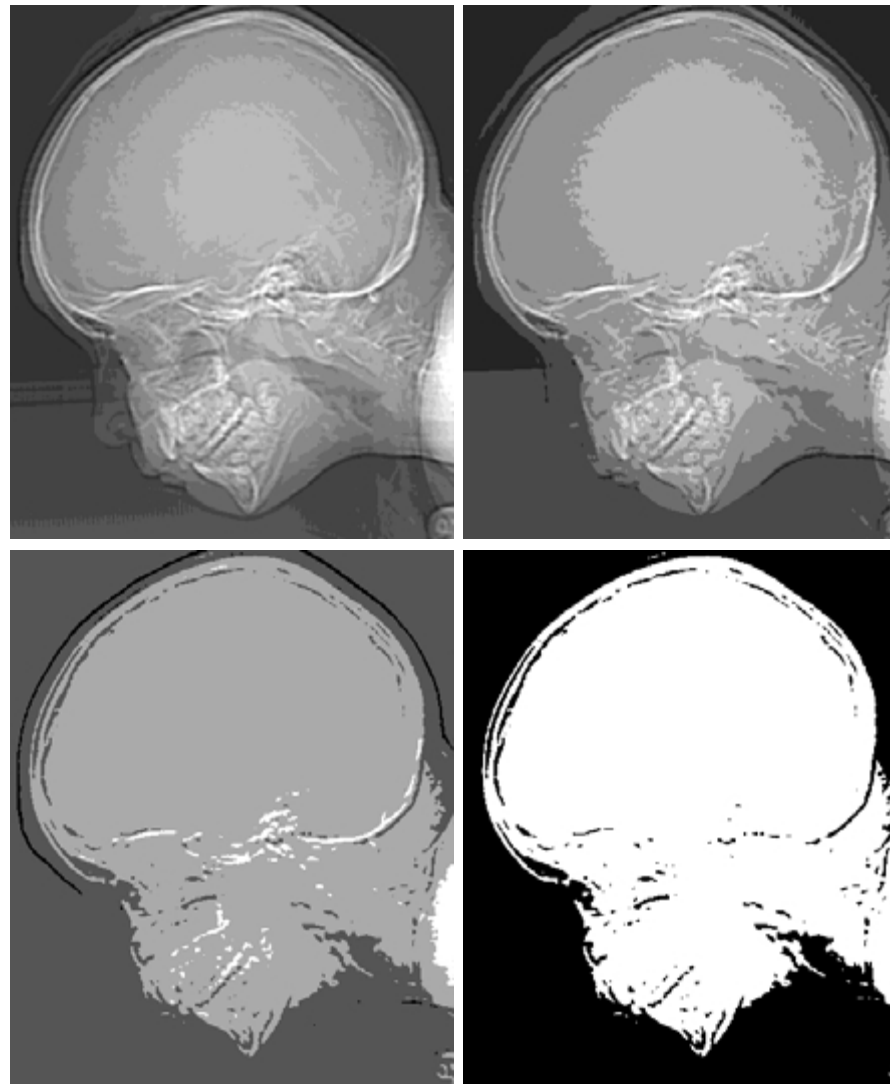

e f
g h

FIGURE 2.21
(Continued)
(e)–(g) Image displayed in 16, 8, 4, and 2 gray levels. (Original courtesy of Dr. David R. Pickens, Department of Radiology & Radiological Sciences, Vanderbilt University Medical Center.)

As a very rough rule of thumb, and assuming powers of 2 for convenience, images of size 256 × 256 pixels and 64 gray levels are about the smallest images that can be expected to be reasonably free of objectionable sampling checkerboards and false contouring. ■

The results in Examples 2.2 and 2.3 illustrate the effects produced on image quality by varying N and k independently. However, these results only partially answer the question of how varying N and k affect images because we have not considered yet any relationships that might exist between these two parameters. An early study by Huang [1965] attempted to quantify experimentally the effects on image quality produced by varying N and k simultaneously. The experiment consisted of a set of subjective tests. Images similar to those shown in Fig. 2.22 were used. The woman's face is representative of an image with relatively little detail; the picture of the cameraman contains an intermediate amount of detail; and the crowd picture contains, by comparison, a large amount of detail.

Sets of these three types of images were generated by varying N and k, and observers were then asked to rank them according to their subjective quality. Results were summarized in the form of so-called *isopreference curves* in the Nk-plane (Fig. 2.23 shows average isopreference curves representative of curves corresponding to the images shown in Fig. 2.22). Each point in the Nk-plane represents an image having values of N and k equal to the coordinates of that point. Points lying on an isopreference curve correspond to images of equal subjective quality. It was found in the course of the experiments that the isopreference curves tended to shift right and upward, but their shapes in each of the three image categories were similar to those shown in Fig. 2.23. This is not unexpected, since a shift up and right in the curves simply means larger values for N and k, which implies better picture quality.

The key point of interest in the context of the present discussion is that isopreference curves tend to become more vertical as the detail in the image increases. This result suggests that for images with a large amount of detail only

a b c

FIGURE 2.22 (a) Image with a low level of detail. (b) Image with a medium level of detail. (c) Image with a relatively large amount of detail. (Image (b) courtesy of the Massachusetts Institute of Technology.)

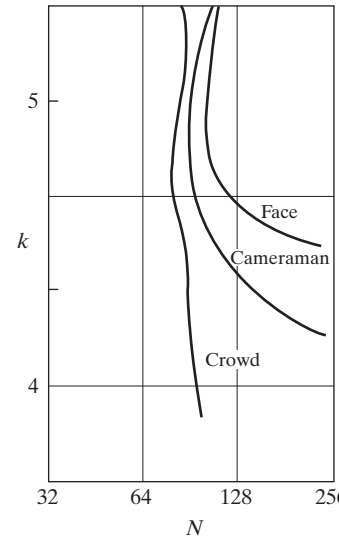

FIGURE 2.23 Representative isopreference curves for the three types of images in Fig. 2.22.

a few gray levels may be needed. For example, the isopreference curve in Fig. 2.23 corresponding to the crowd is nearly vertical. This indicates that, for a fixed value of N, the perceived quality for this type of image is nearly independent of the number of gray levels used (for the range of gray levels shown in Fig. 2.23). It is also of interest to note that perceived quality in the other two image categories remained the same in some intervals in which the spatial resolution was increased, but the number of gray levels actually decreased. The most likely reason for this result is that a decrease in k tends to increase the apparent contrast of an image, a visual effect that humans often perceive as improved quality in an image.

2.4.4 Aliasing and Moiré Patterns

As discussed in more detail in Chapter 4, functions whose area under the curve is finite can be represented in terms of sines and cosines of various frequencies. The sine/cosine component with the highest frequency determines the highest "frequency content" of the function. Suppose that this highest frequency is finite and that the function is of unlimited duration (these functions are called *band-limited functions*). Then, the Shannon sampling theorem [Bracewell (1995)] tells us that, if the function is sampled at a rate equal to or greater than twice its highest frequency, it is possible to recover completely the original function from its samples. If the function is *undersampled*, then a phenomenon called *aliasing* corrupts the sampled image. The corruption is in the form of additional frequency components being introduced into the sampled function. These are called *aliased frequencies*. Note that the *sampling rate* in images is the number of samples taken (in both spatial directions) per unit distance.

As it turns out, except for a special case discussed in the following paragraph, it is impossible to satisfy the sampling theorem in practice. We can only work with sampled data that are finite in duration. We can model the process of convert-

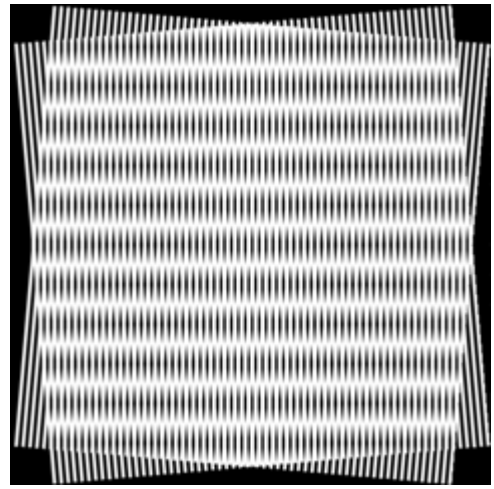

FIGURE 2.24 Illustration of the Moiré pattern effect.

ing a function of unlimited duration into a function of finite duration simply by multiplying the unlimited function by a "gating function" that is valued 1 for some interval and 0 elsewhere. Unfortunately, this function itself has frequency components that extend to infinity. Thus, the very act of limiting the duration of a band-limited function causes it to cease being band limited, which causes it to violate the key condition of the sampling theorem. The principal approach for reducing the aliasing effects on an image is to reduce its high-frequency components by blurring the image (we discuss blurring in detail in Chapter 4) *prior* to sampling. However, aliasing is always present in a sampled image. The effect of aliased frequencies can be seen under the right conditions in the form of so-called *Moiré patterns*[†], as discussed next.

There is one special case of significant importance in which a function of infinite duration can be sampled over a finite interval without violating the sampling theorem. When a function is periodic, it may be sampled at a rate equal to or exceeding twice its highest frequency, and it is possible to recover the function from its samples *provided* that the sampling captures *exactly* an integer number of periods of the function. This special case allows us to illustrate vividly the Moiré effect. Figure 2.24 shows two identical periodic patterns of equally spaced vertical bars, rotated in opposite directions and then superimposed on each other by multiplying the two images. A Moiré pattern, caused by a breakup of the periodicity, is seen in Fig. 2.24 as a 2-D sinusoidal (aliased) waveform (which looks like a corrugated tin roof) running in a vertical direction. A similar pattern can appear when images are digitized (e.g., scanned) from a printed page, which consists of periodic ink dots.

[†] The word *Moiré* appears to have originated with weavers and comes from the word *mohair*, a cloth made from Angora goat hairs.

2.4.5 Zooming and Shrinking Digital Images

We conclude the treatment of sampling and quantization with a brief discussion on how to zoom and shrink a digital image. This topic is related to image sampling and quantization because zooming may be viewed as oversampling, while shrinking may be viewed as undersampling. The key difference between these two operations and sampling and quantizing an original continuous image is that zooming and shrinking are applied to a *digital* image.

Zooming requires two steps: the creation of new pixel locations, and the assignment of gray levels to those new locations. Let us start with a simple example. Suppose that we have an image of size 500×500 pixels and we want to enlarge it 1.5 times to 750×750 pixels. Conceptually, one of the easiest ways to visualize zooming is laying an imaginary 750×750 grid over the original image. Obviously, the spacing in the grid would be less than one pixel because we are fitting it over a smaller image. In order to perform gray-level assignment for any point in the overlay, we look for the closest pixel in the original image and assign its gray level to the new pixel in the grid. When we are done with all points in the overlay grid, we simply expand it to the original specified size to obtain the zoomed image. This method of gray-level assignment is called *nearest neighbor interpolation*. (Pixel neighborhoods are discussed in the next section.)

Pixel replication, the method used to generate Figs. 2.20(b) through (f), is a special case of nearest neighbor interpolation. Pixel replication is applicable when we want to increase the size of an image an integer number of times. For instance, to double the size of an image, we can duplicate each column. This doubles the image size in the horizontal direction. Then, we duplicate each row of the enlarged image to double the size in the vertical direction. The same procedure is used to enlarge the image by any integer number of times (triple, quadruple, and so on). Duplication is just done the required number of times to achieve the desired size. The gray-level assignment of each pixel is predetermined by the fact that new locations are exact duplicates of old locations.

Although nearest neighbor interpolation is fast, it has the undesirable feature that it produces a checkerboard effect that is particularly objectionable at high factors of magnification. Figures 2.20(e) and (f) are good examples of this. A slightly more sophisticated way of accomplishing gray-level assignments is *bilinear interpolation* using the four nearest neighbors of a point. Let (x', y') denote the coordinates of a point in the zoomed image (think of it as a point on the grid described previously), and let $v(x', y')$ denote the gray level assigned to it. For bilinear interpolation, the assigned gray level is given by

$$v(x', y') = ax' + by' + cx'y' + d \tag{2.4-6}$$

where the four coefficients are determined from the four equations in four unknowns that can be written using the four nearest neighbors of point (x', y').

Image shrinking is done in a similar manner as just described for zooming. The equivalent process of pixel replication is row-column deletion. For example, to shrink an image by one-half, we delete every other row and column. We can use the zooming grid analogy to visualize the concept of shrinking by a noninteger factor, except

that we now *expand* the grid to fit over the original image, do gray-level nearest neighbor or bilinear interpolation, and then shrink the grid back to its original specified size. To reduce possible aliasing effects, it is a good idea to blur an image slightly before shrinking it. Blurring of digital images is discussed in Chapters 3 and 4.

It is possible to use more neighbors for interpolation. Using more neighbors implies fitting the points with a more complex surface, which generally gives smoother results. This is an exceptionally important consideration in image generation for 3-D graphics [Watt (1993)] and in medical image processing [Lehmann et al. (1999)], but the extra computational burden seldom is justifiable for general-purpose digital image zooming and shrinking, where bilinear interpolation generally is the method of choice.

EXAMPLE 2.4: Image zooming using bilinear interpolation.

■ Figures 2.20(d) through (f) are shown again in the top row of Fig. 2.25. As noted earlier, these images were zoomed from 128×128, 64×64, and 32×32 to 1024×1024 pixels using nearest neighbor interpolation. The equivalent results using bilinear interpolation are shown in the second row of Fig. 2.25. The improvements in overall appearance are clear, especially in the 128×128 and

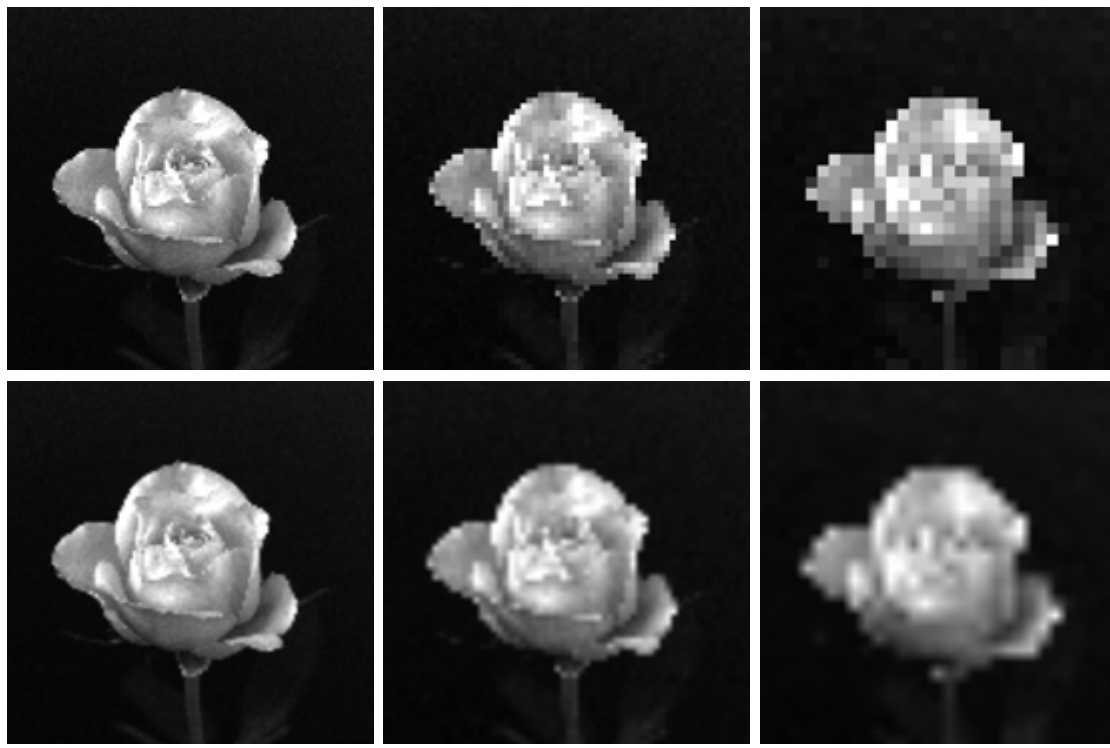

a b c
d e f

FIGURE 2.25 Top row: images zoomed from 128×128, 64×64, and 32×32 pixels to 1024×1024 pixels, using nearest neighbor gray-level interpolation. Bottom row: same sequence, but using bilinear interpolation.

64 × 64 cases. The 32 × 32 to 1024 × 1024 image is blurry, but keep in mind that this image was zoomed by a factor of 32. In spite of this, the result of bilinear interpolation shown in Fig. 2.25(f) is a reasonably good rendition of the original image shape, something that is lost in Fig. 2.25(c). ■

2.5 Some Basic Relationships Between Pixels

In this section, we consider several important relationships between pixels in a digital image. As mentioned before, an image is denoted by $f(x, y)$. When referring in this section to a particular pixel, we use lowercase letters, such as p and q.

2.5.1 Neighbors of a Pixel

A pixel p at coordinates (x, y) has four *horizontal* and *vertical* neighbors whose coordinates are given by

$$(x + 1, y), (x - 1, y), (x, y + 1), (x, y - 1)$$

This set of pixels, called the 4-*neighbors* of p, is denoted by $N_4(p)$. Each pixel is a unit distance from (x, y), and some of the neighbors of p lie outside the digital image if (x, y) is on the border of the image.

The four *diagonal* neighbors of p have coordinates

$$(x + 1, y + 1), (x + 1, y - 1), (x - 1, y + 1), (x - 1, y - 1)$$

and are denoted by $N_D(p)$. These points, together with the 4-neighbors, are called the 8-*neighbors* of p, denoted by $N_8(p)$. As before, some of the points in $N_D(p)$ and $N_8(p)$ fall outside the image if (x, y) is on the border of the image.

2.5.2 Adjacency, Connectivity, Regions, and Boundaries

Connectivity between pixels is a fundamental concept that simplifies the definition of numerous digital image concepts, such as regions and boundaries. To establish if two pixels are connected, it must be determined if they are neighbors and if their gray levels satisfy a specified criterion of similarity (say, if their gray levels are equal). For instance, in a binary image with values 0 and 1, two pixels may be 4-neighbors, but they are said to be connected only if they have the same value.

Let V be the set of gray-level values used to define adjacency. In a binary image, $V = \{1\}$ if we are referring to adjacency of pixels with value 1. In a grayscale image, the idea is the same, but set V typically contains more elements. For example, in the adjacency of pixels with a range of possible gray-level values 0 to 255, set V could be any subset of these 256 values. We consider three types of adjacency:

(a) 4-*adjacency*. Two pixels p and q with values from V are 4-adjacent if q is in the set $N_4(p)$.

(b) 8-*adjacency*. Two pixels p and q with values from V are 8-adjacent if q is in the set $N_8(p)$.

(c) *m-adjacency* (mixed adjacency). Two pixels p and q with values from V are m-adjacent if

(i) q is in $N_4(p)$, *or*

(ii) q is in $N_D(p)$ *and* the set $N_4(p) \cap N_4(q)$ has no pixels whose values are from V.

Mixed adjacency is a modification of 8-adjacency. It is introduced to eliminate the ambiguities that often arise when 8-adjacency is used. For example, consider the pixel arrangement shown in Fig. 2.26(a) for $V = \{1\}$. The three pixels at the top of Fig. 2.26(b) show multiple (ambiguous) 8-adjacency, as indicated by the dashed lines. This ambiguity is removed by using m-adjacency, as shown in Fig. 2.26(c). Two image subsets S_1 and S_2 are adjacent if some pixel in S_1 is adjacent to some pixel in S_2. It is understood here and in the following definitions that *adjacent* means 4-, 8-, or m-adjacent.

A (*digital*) *path* (or *curve*) from pixel p with coordinates (x, y) to pixel q with coordinates (s, t) is a sequence of distinct pixels with coordinates

$$(x_0, y_0), (x_1, y_1), \ldots, (x_n, y_n)$$

where $(x_0, y_0) = (x, y)$, $(x_n, y_n) = (s, t)$, and pixels (x_i, y_i) and (x_{i-1}, y_{i-1}) are adjacent for $1 \leq i \leq n$. In this case, n is the *length* of the path. If $(x_0, y_0) = (x_n, y_n)$, the path is a *closed* path. We can define 4-, 8-, or m-paths depending on the type of adjacency specified. For example, the paths shown in Fig. 2.26(b) between the northeast and southeast points are 8-paths, and the path in Fig. 2.26(c) is an m-path. Note the absence of ambiguity in the m-path.

Let S represent a subset of pixels in an image. Two pixels p and q are said to be *connected* in S if there exists a path between them consisting entirely of pixels in S. For any pixel p in S, the *set* of pixels that are connected to it in S is called a *connected component* of S. If it only has one connected component, then set S is called a *connected set*.

Let R be a subset of pixels in an image. We call R a *region* of the image if R is a connected set. The *boundary* (also called *border* or *contour*) of a region R is the set of pixels in the region that have one or more neighbors that are not in R. If R happens to be an entire image (which we recall is a rectangular set of pixels), then its boundary is defined as the set of pixels in the first and last rows and columns of the image. This extra definition is required because an image has no neighbors beyond its border. Normally, when we refer to a region, we are

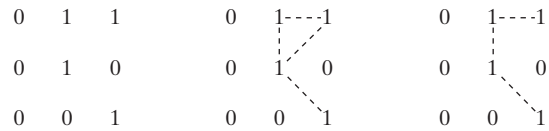

a b c

FIGURE 2.26 (a) Arrangement of pixels; (b) pixels that are 8-adjacent (shown dashed) to the center pixel; (c) m-adjacency.

referring to a subset of an image, and any pixels in the boundary of the region that happen to coincide with the border of the image are included implicitly as part of the region boundary.

The concept of an *edge* is found frequently in discussions dealing with regions and boundaries. There is a key difference between these concepts, however. The boundary of a finite region forms a closed path (Problem 2.14) and is thus a "global" concept. As discussed in detail in Chapter 10, edges are formed from pixels with derivative values that exceed a preset threshold. Thus, the idea of an edge is a "local" concept that is based on a measure of gray-level discontinuity at a point. It is possible to link edge points into edge segments, and sometimes these segments are linked in such a way that correspond to boundaries, but this is not always the case. The one exception in which edges and boundaries correspond is in binary images. Depending on the type of connectivity and edge operators used (we discuss these in Chapter 10), the edge extracted from a binary region will be the same as the region boundary. This is intuitive. Conceptually, until we arrive at Chapter 10, it is helpful to think of edges as intensity discontinuities and boundaries as closed paths.

2.5.3 Distance Measures

For pixels p, q, and z, with coordinates (x, y), (s, t), and (v, w), respectively, D is a *distance function* or *metric* if

(a) $D(p, q) \geq 0 \quad (D(p, q) = 0 \quad \text{iff} \quad p = q)$,
(b) $D(p, q) = D(q, p)$, and
(c) $D(p, z) \leq D(p, q) + D(q, z)$.

The *Euclidean distance* between p and q is defined as

$$D_e(p, q) = \left[(x - s)^2 + (y - t)^2\right]^{\frac{1}{2}}. \tag{2.5-1}$$

For this distance measure, the pixels having a distance less than or equal to some value r from (x, y) are the points contained in a disk of radius r centered at (x, y).

The D_4 *distance* (also called *city-block distance*) between p and q is defined as

$$D_4(p, q) = |x - s| + |y - t|. \tag{2.5-2}$$

In this case, the pixels having a D_4 distance from (x, y) less than or equal to some value r form a diamond centered at (x, y). For example, the pixels with D_4 distance ≤ 2 from (x, y) (the center point) form the following contours of constant distance:

$$\begin{array}{ccccc} & & 2 & & \\ & 2 & 1 & 2 & \\ 2 & 1 & 0 & 1 & 2 \\ & 2 & 1 & 2 & \\ & & 2 & & \end{array}$$

The pixels with $D_4 = 1$ are the 4-neighbors of (x, y).

The D_8 *distance* (also called *chessboard distance*) between p and q is defined as

$$D_8(p, q) = \max(|x - s|, |y - t|). \tag{2.5-3}$$

In this case, the pixels with D_8 distance from (x, y) less than or equal to some value r form a square centered at (x, y). For example, the pixels with D_8 distance ≤ 2 from (x, y) (the center point) form the following contours of constant distance:

$$\begin{matrix} 2 & 2 & 2 & 2 & 2 \\ 2 & 1 & 1 & 1 & 2 \\ 2 & 1 & 0 & 1 & 2 \\ 2 & 1 & 1 & 1 & 2 \\ 2 & 2 & 2 & 2 & 2 \end{matrix}$$

The pixels with $D_8 = 1$ are the 8-neighbors of (x, y).

Note that the D_4 and D_8 distances between p and q are independent of any paths that might exist between the points because these distances involve only the coordinates of the points. If we elect to consider m-adjacency, however, the D_m distance between two points is defined as the shortest m-path between the points. In this case, the distance between two pixels will depend on the values of the pixels along the path, as well as the values of their neighbors. For instance, consider the following arrangement of pixels and assume that p, p_2, and p_4 have value 1 and that p_1 and p_3 can have a value of 0 or 1:

$$\begin{matrix} & p_3 & p_4 \\ p_1 & p_2 & \\ p & & \end{matrix}$$

Suppose that we consider adjacency of pixels valued 1 (i.e., $V = \{1\}$). If p_1 and p_3 are 0, the length of the shortest m-path (the D_m distance) between p and p_4 is 2. If p_1 is 1, then p_2 and p will no longer be m-adjacent (see the definition of m-adjacency) and the length of the shortest m-path becomes 3 (the path goes through the points $pp_1p_2p_4$). Similar comments apply if p_3 is 1 (and p_1 is 0); in this case, the length of the shortest m-path also is 3. Finally, if both p_1 and p_3 are 1 the length of the shortest m-path between p and p_4 is 4. In this case, the path goes through the sequence of points $pp_1p_2p_3p_4$.

2.5.4 Image Operations on a Pixel Basis

Numerous references are made in the following chapters to operations between images, such as dividing one image by another. In Eq. (2.4-2), images were represented in the form of matrices. As we know, matrix division is not defined. However, when we refer to an operation like "dividing one image by another," we mean specifically that the division is carried out between *corresponding* pixels in the two images. Thus, for example, if f and g are images, the first element of the image formed by "dividing" f by g is simply the first pixel in f divided by the first pixel in g; of course, the assumption is that none of the pixels in g have value 0. Other arithmetic and logic operations are similarly defined between corresponding pixels in the images involved.

2.6 Linear and Nonlinear Operations

Let H be an operator whose input and output are images. H is said to be a *linear* operator if, for any two images f and g and any two scalars a and b,

$$H(af + bg) = aH(f) + bH(g). \tag{2.6-1}$$

In other words, the result of applying a linear operator to the sum of two images (that have been multiplied by the constants shown) is identical to applying the operator to the images individually, multiplying the results by the appropriate constants, and then adding those results. For example, an operator whose function is to compute the sum of K images is a linear operator. An operator that computes the absolute value of the difference of two images is not. An operator that fails the test of Eq. (2.6-1) is by definition *nonlinear*.

Linear operations are exceptionally important in image processing because they are based on a significant body of well-understood theoretical and practical results. Although nonlinear operations sometimes offer better performance, they are not always predictable, and for the most part are not well understood theoretically.

Summary

The material in this chapter is primarily background information for subsequent discussions. Our treatment of the human visual system, although brief, provides a basic idea of the capabilities of the eye in perceiving pictorial information. The discussion of light and the electromagnetic spectrum is fundamental in understanding the origin of the many images we use in this book. Similarly, the image model developed in Section 2.3.4 is used in the Chapter 4 as the basis for an image enhancement technique called *homomorphic filtering*, and again in Chapter 10 to explain the effect of illumination on the shape of image histograms.

The sampling ideas introduced in Section 2.4 are the foundation for many of the digitizing phenomena likely to be encountered in practice. These ideas can be expanded further once a basic understanding of frequency content is mastered. A detailed discussion of the frequency domain is given in Chapter 4. The concepts of sampling and aliasing effects also are of importance in the context of image acquisition.

The concepts introduced in Section 2.5 are the basic building blocks for processing techniques based on pixel neighborhoods. As shown in the following chapter and in Chapter 5, neighborhood processing methods are at the core of many image enhancement and restoration procedures. When applicable, neighborhood processing is favored in commercial applications of image processing due to their operational speed and simplicity of implementation in hardware and/or firmware. Finally, the concept of a linear operator and the theoretical and conceptual power associated with it will be used extensively in the following three chapters.

References and Further Reading

Additional reading for the material in Section 2.1 regarding the structure of the human eye may be found in Atchison and Smith [2000], and Oyster [1999]. For additional reading on visual perception, see Regan [2000] and Gordon [1997]. The book by Hubel [1988] and the now classic book by Cornsweet [1970] also are of interest. Born and Wolf [1999]

is a basic reference that discusses light in terms of electromagnetic theory. Electromagnetic energy propagation is covered in some detail by Felsen and Marcuvitz [1994].

The area of image sensing is quite broad and very fast moving. An excellent source of information on optical and other imaging sensors is the International Society for Optical Engineering (SPIE). The following are representative publications by the SPIE in this area: Blouke et al. [2001], Hoover and Doty [1996], and Freeman [1987].

The image model presented in Section 2.3.4 is from Oppenheim, Schafer, and Stockham [1968]. A reference for the illumination and reflectance values used in that section is the *IES Lighting Handbook* [2000]. For additional reading on image sampling and some of its effects, such as aliasing, see Bracewell [1995]. The early experiments mentioned in Section 2.4.3 on perceived image quality as a function of sampling and quatization were reported by Huang [1965]. The issue of reducing the number of samples and gray levels in an image while minimizing the ensuing degradation is still of current interest, as exemplified by Papamarkos and Atsalakis [2000]. For further reading on image shrinking and zooming, see Sid-Ahmed [1995], Unser et al. [1995], Umbaugh [1998], and Lehmann et al. [1999]. For further reading on the topics covered in Section 2.5, see Rosenfeld and Kak [1982], Marchand-Maillet and Sharaiha [2000], and Ritter and Wilson [2001]. Additional reading on linear systems in the context of image processing may be found in Castleman [1996].

Problems

See inside front cover

Detailed solutions to the problems marked with a star can be found in the book web site. The site also contains suggested projects based on the material in this chapter.

★2.1 Using the background information provided in Section 2.1, and thinking purely in geometric terms, estimate the diameter of the smallest printed dot that the eye can discern if the page on which the dot is printed is 0.2 m away from the eyes. Assume for simplicity that the visual system ceases to detect the dot when the image of the dot on the fovea becomes smaller than the diameter of one receptor (cone) in that area of the retina. Assume further that the fovea can be modeled as a square array of dimensions 1.5 mm $\times$ 1.5 mm, and that the cones and spaces between the cones are distributed uniformly throughout this array.

2.2 When you enter a dark theater on a bright day, it takes an appreciable interval of time before you can see well enough to find an empty seat. Which of the visual processes explained in Section 2.1 is at play in this situation?

★2.3 Although it is not shown in Fig. 2.10, alternating current certainly is part of the electromagnetic spectrum. Commercial alternating current in the United States has a frequency of 60 Hz. What is the wavelength in kilometers of this component of the spectrum?

2.4 You are hired to design the front end of an imaging system for studying the boundary shapes of cells, bacteria, viruses, and protein. The front end consists, in this case, of the illumination source(s) and corresponding imaging camera(s). The diameters of circles required to enclose individual specimens in each of these categories are 50, 1, 0.1, and 0.01 μm, respectively.

(a) Can you solve the imaging aspects of this problem with a single sensor and camera? If your answer is yes, specify the illumination wavelength band and the type of camera needed. Identify the camera as being a color camera, far-infrared camera, or whatever appropriate name corresponds to the illumination source.

(b) If your answer in (a) is no, what type of illumination sources and corresponding imaging sensors would you recommend? Specify the light sources